AD_____

Award Number: W81XWH-06-1-0459

TITLE: New Approaches for Prostate Cancer Combination Therapy

PRINCIPAL INVESTIGATOR: Luiz F. Zerbini, Ph.D.

CONTRACTING ORGANIZATION: Beth Israel Deaconess Medical Center
Boston, MA 02215

REPORT DATE: April 2009

TYPE OF REPORT: Final

PREPARED FOR: U.S. Army Medical Research and Materiel Command
Fort Detrick, Maryland 21702-5012

REPORT DOCUMENTATION PAGE

Form Approved
OMB No. 0704-0188

1. REPORT DATE	2. REPORT TYPE	3. DATES COVERED
01-04-2009	Final	20 MAR 2006 - 19 MAR 2009

4. TITLE AND SUBTITLE
New Approaches for Prostate Cancer Combination Therapy

5a. CONTRACT NUMBER

5b. GRANT NUMBER
W81XWH-06-1-0459

5c. PROGRAM ELEMENT NUMBER

6. AUTHOR(S)
Luiz F. Zerbini, Ph.D.

Email: lzerbini@bidmc.harvard.edu

5d. PROJECT NUMBER

5e. TASK NUMBER

5f. WORK UNIT NUMBER

7. PERFORMING ORGANIZATION NAME(S) AND ADDRESS(ES)

Beth Israel Deaconess Medical Center
Boston, MA 02215

8. PERFORMING ORGANIZATION REPORT NUMBER

9. SPONSORING / MONITORING AGENCY NAME(S) AND ADDRESS(ES)
U.S. Army Medical Research and Materiel Command
Fort Detrick, Maryland 21702-5012

10. SPONSOR/MONITOR'S ACRONYM(S)

11. SPONSOR/MONITOR'S REPORT NUMBER(S)

12. DISTRIBUTION / AVAILABILITY STATEMENT
Approved for Public Release; Distribution Unlimited

13. SUPPLEMENTARY NOTES

14. ABSTRACT

The mechanisms underlying the antineoplastic actions of NSAIDs remain poorly understood. We started deciphering now the mechanisms by which NSAIDs induce programmed cell death and growth arrest in cancer. In this report we show that induction of the pro-apoptotic cytokine melanoma differentiation associated gene-7/Interleukin-24 (MDA-7/IL-24) and the expression of growth arrest and DNA damage inducible (GADD) 45 α and γ by several NSAIDs is an essential step for G2/M growth arrest and apoptosis induction of cancer cells and inhibition of tumor growth in vivo. MDA-7/IL24 dependent upregulation of GADD45 α and γ expression is sufficient for cancer cell apoptosis, since inhibition of GADD45α and γ by small interfering RNA abrogates apoptosis and growth arrest induction by the NSAID, blocks JNK activation and restores CDC2 kinase activity. Our results establish MDA-7/IL-24 and GADD45α and γ as critical mediators of apoptosis and growth arrest in response to NSAIDs in cancer cells. Pharmacological inhibitors of NF-κB have a potent effect in apoptosis induction of prostate cancer cells as well as in combination with NSAIDs. This new treatment could be then tested in combination of inhibitors of NF-κB pathway which are already in clinical trials.

15. SUBJECT TERMS
Sulindac sulfide, NSAIDs, apoptosis, pharmacological inhibitors of NF-κB, combinatorial treatment

16. SECURITY CLASSIFICATION OF:			17. LIMITATION OF ABSTRACT	18. NUMBER OF PAGES	19a. NAME OF RESPONSIBLE PERSON
a. REPORT	b. ABSTRACT	c. THIS PAGE			USAMRMC
U	U	U	UU	34	19b. TELEPHONE NUMBER *(include area code)*

Table of Contents

Page

Introduction

An increasing number of studies have demonstrated that some non-steroidal anti-inflammatory drugs (NSAIDs) such as Sulindac sulfide, at clinically tolerable concentrations, are effective in the treatment of several types of cancer. Sulindac sulfide has been shown to reduce CaP proliferation and induce CaP apoptosis in vitro and in vivo. Nevertheless, the mechanism of apoptosis induction is poorly understood and more studies are needed to fully elucidate the molecular and biochemical pathways of Sulindac-induced apoptosis. Our notion is that by dissecting the molecular mechanisms of CaP apoptosis induction by Sulindac sulfide and of a whole panel of NSAIDs with potential anti-prostate cancer activities we may be able to rationally design a combination of several NSAIDs with distinct target specificities that should act synergistically and, thus, more effectively against CaP. Our goal is to systematically decipher the pathways that are involved in apoptosis induction by Sulindac sulfide with particular emphasis on the role of GADD45 α and γ, IL-24 and JNK kinase. Our hypothesis is that the detailed pathways will provide a multitude of novel entry points for targeted drug development, towards drugs specific for CaP apoptosis induction without the adverse reactions of current NSAIDs.

Body

Based on the approved Statement of Work the following research accomplishments are associated with each task outlined below:

Aim 1. Determine the role of the GADD45 family, JNK and other apoptosis and cell cycle related proteins in Sulindac mediated apoptosis of CaP (1-18 months)

Multiple NSAIDs are potent inducers of apoptosis in prostate cancer cells. A broad panel of NSAIDs was tested for their abilities to induce apoptosis in cancer cells. The concentrations for all NSAIDs drugs used in this study were selected carefully and comparable to the achievable plasma concentrations (1-3). However, some drug concentrations exceeded thephysiologically achievable doses (1-3). Apoptosis was measured 24 and 48 hours after treatment of DU145 prostate cancer cells with this set of NSAIDs, revealing that a variety of, but not all NSAIDs induced apoptosis in DU145 cells. Strong inducers of apoptosis included Sulindac sulfide, Finasteride, Diclofenac, Flufenamic acid, Flurbiprofen, Sulindac sulfone and NS-398 when compared with the solvent controls, whereas treatment with Aspirin, Celocoxib, Acetaminophen, Ibuprofen, Naproxen, Meloxican and Ebselen resulted only in marginal apoptosis induction (see Fig. 1 in the manuscript Zerbini *et al*. Cancer Research 66: 11922-31, 2006 in the appendices section). Sulindac sulfide was the strongest inducer of apoptosis in prostate cancer cells. Sulindac sulfide treatment also induced G2/M growth arrest in prostate cancer cell lines when compared to control by increasing the fraction of cells in the G2/M phase by 2fold (2,3).

It has been established that Sulindac sulfide reaches peak plasma concentrations of 30-50µM (2,3), coming down to a steady state plasma concentration of 5-10µM (4). We, therefore, decide to evaluate whether the sulindac sulfide steady plasma concentration achievable in patients (4) is still able to induce apoptosis in cancer cells. Prostate cancer cells were treated with 5, 10, 25 and 50µM of Sulindac sulfide and apoptosis was measured 24 hours post-treatment. We demonstrate that even low concentrations as 5-10µM Sulindac sulfide are sufficient to induce apoptosis in cancer cells (see supplementary Figure 4A in the manuscript Zerbini *et al*. Cancer Research 66: 11922-31, 2006 in the appendices section).

Our transcriptional profiling experiments, moreover, demonstrated a strong upregulation of GADD45α up to 16-fold by Sulindac sulfide (see supplementary Table 1 in the manuscript Zerbini *et al*. Cancer Research 66: 11922-31, 2006 in the appendices section). The GADD45

gene family encodes three structurally highly related growth arrest- and DNA damage-inducible proteins, GADD45α, β and γ (5) that play a role in the G2/M checkpoint in response to DNA damage (6). To evaluate whether regulation of GADD45 genes is involved in NSAID-mediated apoptosis, expression of GADD45 family members was measured by real time PCR in the different cancer cell lines treated with Sulindac sulfide (see Fig. 4A in the manuscript Zerbini *et al*. Cancer Research 66: 11922-31, 2006 in the appendices section). Whereas GADD45β expression was not significantly affected by Sulindac sulfide in any of the cell lines, the drug induced GADD45α and γ expression 1.5-27-fold in the various cancer cell types, indicating that GADD45α and γ expression is consistently regulated by Sulindac sulfide (see in the manuscript Zerbini *et al*. Cancer Research 66: 11922-31, 2006 in the appendices section Fig. 4A). Interestingly, the correlation between induction of GADD45α and γ was significant (Correlation coefficient 0.85; p value=0.0001).

Differences in mRNA expression of the GADD45 family members were corroborated on the protein level by Western blot analysis using protein extracts from DU145 and PC-3 cells treated with Sulindac sulfide for 24 hours. GADD45α and γ, but not β protein expression were induced in Sulindac sulfide treated cancer cells (see Fig. 4B in the manuscript Zerbini *et al*. Cancer Research 66: 11922-31, 2006 in the appendices section).

a) **Determine whether JNK kinase activation by Sulindac is GADD45 α, β or γ dependent** – (Months1-4)

The importance of GADD45α and γ for NSAID-induced JNK activation was evaluated in DU145 and PC-3 cells infected with the GADD45α or γ siRNA lentiviruses or the control lentivirus and treated with Sulindac sulfide for 24 hours. siRNA mediated inhibition of Sulindac sulfide-mediated upregulation of GADD45α and γ expression drastically reduced JNK activation in both cell lines, correlating with the inhibition of apoptosis induction (see Fig. 6D in the manuscript Zerbini *et al*. Cancer Research 66: 11922-31, 2006 in the appendices section).

To establish the relevance of JNK activation in mediating apoptosis in cancer cells, apoptosis was measured in protein extracts obtained from DU145 and PC-3 cells treated with 50 μM of Sulindac sulfide or DMSO in the absence or presence of a specific JNK inhibitor, JNKII. Compared to the control, apoptosis of Sulindac sulfide treated cells was reduced by more than 56% in DU145 cells and 40% in PC-3 cells in JNK II treated cells, but inhibition of JNK did not fully abolish apoptosis induction (see Fig. 6E in the manuscript Zerbini *et al*. Cancer Research 66: 11922-31, 2006 in the appendices section). These results suggest that JNK contributes to, but is not absolutely essential for Sulindac sulfide-mediated apoptosis.

b) **Determine whether inhibition of GADD45 family genes and JNK affects cell cycle, proliferation and/or apoptosis in CaP treated with Sulindac** –(Months 1-8)

NSAID-mediated GADD45α and γ induction is essential for CDK1/cdc2 kinase activation and growth arrest. Our transcriptional profiling analysis demonstrated that in concordance with the observed G2/M cell cycle arrest induced by Sulindac sulfide, several genes involved in the G2/M checkpoint and CDK1/cdc2 kinase regulation are downregulated by Sulindac sulfide including cdc25C, Cdk1/cdc2, cyclin B1, and cyclin B2, whereas the cyclin dependent kinase inhibitor p21 is upregulated (see supplementary Table 1 in the manuscript Zerbini *et al*. Cancer Research 66: 11922-31, 2006 in the appendices section). Western blot analysis of protein extracts from DU145 and PC-3 cells treated with Sulindac sulfide for 24 hours corroborated the expression changes on the protein level. Protein expression of cdc-25C, cyclin B1, and cyclin B2 decreased and p21 protein expression increased in response to Sulindac sulfide (see Fig. 5a in the manuscript Zerbini *et al*. Cancer Research 66: 11922-31, 2006 in the appendices section). GADD45α has been shown to inhibit the kinase activity of the Cdc2/CyclinB1 complex (7) and progression from the G2 to the M phase of the cell cycle (8). To determine the role of GADD45α

and GADD45γ in NSAID-induced G2/M arrest, we infected DU145 prostate cancer cells with lentiviruses encoding siRNAs for GADD45α, GADD45γ or GFP. An *in vitro* Cdc2 kinase assay was performed with whole cell lysates from these infected cells after treatment with Sulindac sulfide or DMSO for 24 hours using histone H1 as the Cdc2 substrate. Active Cdc2 directly correlates with enhanced phosphorylation of histone H1. A significant level of phosphorylated histone H1 in untreated cells infected with the control lentivirus indicated significant Cdc2 activity in proliferating DU145 cells (see Fig. 5B in the manuscript Zerbini *et al*. Cancer Research 66: 11922-31, 2006 in the appendices section). Cdc2 activity was substantially decreased 24 hours after Sulindac sulfide treatment correlating with enhanced GADD45α and γ expression and G2/M arrest. However, inhibition of GADD45α and γ expression in DU145 cells by the siRNA lentiviruses restored Cdc2 kinase activity as seen by increased histone H1 phosphorylation (see Fig. 5B in the manuscript Zerbini *et al*. Cancer Research 66: 11922-31, 2006 in the appendices section). These data suggest that Sulindac sulfide induced G2/M cell cycle arrest is due to a combination of decreased expression of several G2/M transition cell cycle regulators and MDA-7/IL-24 induced GADD45α and GADD45γ upregulation that leads to inhibition of Cdc2 activity.

To elucidate the functional relevance of GADD45α and γ for NSAID-mediated apoptosis, we measured apoptosis induction by Sulindac sulfide in GADD45α and γ knockdown cells. siRNA mediated inhibition of Sulindac sulfide induced upregulation of GADD45α or γ expression almost completely abrogated apoptosis induction (see Fig. 6A in the manuscript Zerbini *et al*. Cancer Research 66: 11922-31, 2006 in the appendices section), clearly demonstrating the absolute requirement of MDA-7/IL-24-dependent GADD45α and γ upregulation for apoptosis induction by NSAIDs.

Since we and others had shown that c-jun N-terminal kinase (JNK) activation plays a role in apoptosis induction in cancer cells and GADD45α and γ interact with the upstream kinase of JNK, MEKK4, and activate JNK (5), we evaluated the relevance of JNK for NSAID-mediated apoptosis. JNK kinase activity was tested in protein extracts obtained from DU145 and PC-3 cells treated with Sulindac sulfide or DMSO for 24 hours by an *in vitro* kinase assay. Western blot analysis revealed very little JNK activity in untreated control cells and a strong increase in JNK activity in both cell lines upon treatment with Sulindac sulfide (see Fig. 6B in the manuscript Zerbini *et al*. Cancer Research 66: 11922-31, 2006 in the appendices section).

c) **Determine whether inhibition or overexpression of GADD45 family genes affects tumor formation in SCID mice treated with Sulindac** – (Months 4-18)

To determine whether NSAIDs reduce tumor growth *in vivo* and to evaluate whether their effects may be dependent on induction of GADD45 family genes, prostate cancer cells stably infected with LV-siRNA GFP or LV-siRNA GADD45 α and γ as well as uninfected cells were orthotopically implanted into the prostate of SCID mice. The mice were randomly divided into two groups and fed one of two diets through the entire experiment: AIN-93G as the control and the AIN-93G diet supplemented with 200ppm Sulindac sulfide. Two months later the animals were examined for tumor formation and tumor weight. All mice developed tumors indicating that this particular dose of Sulindac sulfide did not prevent tumor formation. As seen in Figure 3E, infection of DU145 cells with the LV-siRNA GFP virus did not affect tumor growth in the control diet group, since implantation of uninfected DU145 cells showed a similar pattern of tumor growth and tumor weight when compared with the LV-siRNA GFP group (see Fig. 3E in the manuscript Zerbini *et al*. Cancer Research 66: 11922-31, 2006 in the appendices section). Sulindac sulfide treatment reduced the average tumor weight in the LV-siRNA GFP group by 38% when compared to the control diet confirming its anti-tumor efficacy (see Fig. 3E in the manuscript Zerbini *et al*. Cancer Research 66: 11922-31, 2006 in the appendices section).

Although tumor weight increase in the Sulindac sulfide treated LV-siRNA GADD45 α γ group compared with the Sulindac sulfide treated LV-siRNA GFP group (0.487g versus 0.38g), this result was not statistically significant (p=0.0638).

However, the same experiments were done using prostate cancer cells stably infected with LV-siRNA GFP or LV-siRNA IL-24. Surprisingly, the blockage of IL-24 expression by siRNA interference in the LV-siRNA IL24 group strongly enhanced tumor growth demonstrating that the low endogenous basal IL-24 expression acts as a tumor suppressor (p value =0.010) (see Fig. 3E in the manuscript Zerbini *et al*. Cancer Research 66: 11922-31, 2006 in the appendices section). Tumor weight markedly increased by 60% in the LV-siRNA IL24 group fed with the control diet when compared with the LV-siRNA GFP group (0.969g versus 0.623g; p value 0.010).

Sulindac sulfide treatment also reduced tumor growth in the LV-siRNA IL24 group to some extent; however, tumor weight was still 75% higher than the Sulindac-treated LV-siRNA GFP group (p value = 0.024) (see Fig. 3E in the manuscript Zerbini *et al*. Cancer Research 66: 11922-31, 2006 in the appendices section). These results indicate that NSAID-mediated IL-24 induction plays a critical role in tumor growth and also indicate a tumor suppressor activity of IL-24.

Aim 2. Elucidate the precise role of IL-24 in Sulindac mediated apoptosis of CaP (12-24).

a) **Evaluate whether IL-24 is mediating Sulindac triggered apoptosis by RNA interference experiments.** - (Months 12-24)

The pro-apoptotic cytokine MDA-7/IL-24 is the critical mediator of NSAID induced apoptosis and growth arrest in cancer cells and inhibition of tumor growth in vivo. To elucidate the detailed molecular mechanisms underlying NSAIDs-mediated cell cycle arrest and apoptosis in cancer cells, we performed oligonucleotide microarray-based transcriptional profiling of DU145 and PC-3 cells treated with 50μM of Sulindac sulfide vs. DMSO. Detailed bioinformatic analysis revealed that Sulindac sulfide does not trigger indiscriminate transcriptional shutdown of cancer cells, but induces distinct patterns of gene expression changes for a wide range of transcripts related to apoptosis and cell cycle (see supplementary Table 1 in the manuscript Zerbini *et al.* Cancer Research 66: 11922-31, 2006 in the appendices section) that were consistent across the two cell lines, further confirming their apparent relevance for the cell cycle and cell death effects of Sulindac sulfide.

Particularly striking and unanticipated was the dramatic upregulation of the pro-apoptotic cytokine interleukin 24, also named melanoma differentiation associated gene-7 (IL-24 or MDA-7) (9,10). MDA-7/IL-24 was by far the highest upregulated gene in both cell lines (140-fold in PC-3 and 722-fold in DU145). MDA-7/IL-24 has been shown to be a novel tumor suppressor gene (10,11). At low presumably physiological concentrations, MDA-7/IL-24 functions predominantly as a cytokine involved in immune regulation (10,11). However, when overexpressed at supra-physiological levels using an adenovirus vector, MDA-7/IL-24 shows cancer-cell specific growth inhibitory properties without negatively affecting normal cells (10-12). Furthermore, elevated endogenous MDA-7/IL-24 expression correlates with enhanced apoptosis and prolonged overall survival of patients with small cell lung cancer, further supporting the anti-cancer role of MDA-7/IL-24 (13).

To evaluate the functional relevance of MDA-7/IL-24 induction for NSAIDs-mediated apoptosis, we measured mRNA expression levels of MDA-7/IL-24 in response to Sulindac sulfide in the same cancer cell lines tested above for apoptosis induction by Sulindac sulfide. Real time PCR analysis demonstrated that Sulindac sulfide induces MDA-7/IL-24 expression in a variety of cancer types, up to124-fold in DU145 cells and ~10-20-fold in various other cancer cell lines (see Fig. 3a in the manuscript Zerbini *et al.* Cancer Research 66: 11922-31, 2006 in the appendices section). Induction of MDA-7/IL-24 by Sulindac sulfide correlated with the ability of

this drug to induce extensive apoptosis in these cell lines (see Fig. 2A in the manuscript Zerbini *et al.* Cancer Research 66: 11922-31, 2006 in the appendices section). These results indicates that Sulindac sulfide mediated induction of MDA-7/IL-24 expression is a common pathway in various types of cancer cells that respond to this NSAID by undergoing apoptosis and strongly suggest that MDA-7/IL-24 plays a critical role in apoptosis induction.

To evaluate the relationship between MDA-7/IL-24 induction and apoptosis induction by various NSAIDs, we measured mRNA expression levels of MDA-7/IL-24 in response to different NSAIDs in prostate cancer cells. Real time PCR analysis demonstrated that induction of MDA-7/IL-24 is common to NSAIDs that induce apoptosis in cancer cells, since multiple, structurally unrelated NSAIDs strongly induced MDA-7/IL-24 expression in DU145 prostate carcinoma cells (see Fig. 3b in the manuscript Zerbini *et al*. Cancer Research 66: 11922-31, 2006 in the appendices section) in strong correlation with NSAID-mediated apoptosis induction (correlation coefficient 0.91; $p<.0001$). NSAIDs that strongly enhanced apoptosis (see Fig. 1 in the manuscript Zerbini *et al*. Cancer Research 66: 11922-31, 2006 in the appendices section) dramatically induced MDA-7/IL-24 expression (see Fig. 3b in the manuscript Zerbini *et al*. Cancer Research 66: 11922-31, 2006 in the appendices section), whereas NSAIDs that only marginally induced apoptosis (Fig. 1) did not significantly enhance MDA-7/IL-24 expression (see Fig. 3b in the manuscript Zerbini *et al*. Cancer Research 66: 11922-31, 2006 in the appendices section) These data suggest a common mechanism for structurally unrelated NSAIDs in apoptosis induction.

We and others have shown (10-12) that overexpression of MDA-7/IL-24 following infection with an adenovirus carrying the MDA-7/IL-24 gene induces apoptosis and inhibits cell proliferation in cancer cells (14) (see supplementary Fig. 5A and B in the manuscript Zerbini *et al*. Cancer Research 66: 11922-31, 2006 in the appendices section). To determine whether induction of growth arrest and apoptosis in cancer cells by NSAIDs is dependent on MDA-7/IL-24 upregulation, we generated siRNA oligonucleotides and a lentivirus encoding this siRNA against MDA-7/IL-24. The specificity of the MDA-7/IL-24 siRNA oligos was validated as described in supplementary methods and supplementary Fig.5C in the manuscript Zerbini *et al*. Cancer Research 66: 11922-31, 2006 in the appendices section. Infection with the MDA-7/IL-24 siRNA lentivirus reduced apoptosis induced by multiple NSAIDs by 90% (see Fig. 3C in the manuscript Zerbini *et al*. Cancer Research 66: 11922-31, 2006 in the appendices section) and reversed for a large part the G2/M cell cycle arrest (see Fig. 3D in the manuscript Zerbini *et al*. Cancer Research 66: 11922-31, 2006 in the appendices section). These results demonstrate that MDA-7/IL-24 may play an important role in tumor cell survival and, for the first time, implicate MDA-7/IL-24 as an essential mediator of NSAID action in cancer cells.

MDA-7/IL-24 regulates and induces GADD45α and γ without affecting GADD45β expression (14,15) (also see supplementary Fig.6 in the manuscript Zerbini *et al.* Cancer Research 66: 11922-31, 2006 in the appendices section). Furthermore, our data shows that upregulation of GADD45α and γ strongly correlated with the ability of Sulindac sulfide to induce MDA-7/IL-24 expression (Correlation coefficient 0.63; p value=0.016 and correlation coefficient 0.69;p value= 0.0068, respectively) (see Fig. 3A in the manuscript Zerbini *et al.* Cancer Research 66: 11922-31, 2006 in the appendices section).

To evaluate whether NSAID-mediated induction of GADD45α and γ expression is dependent on MDA-7/IL-24 upregulation, we transfected prostate cancer cells with MDA-7/IL-24 siRNA oligonucleotides and measured GADD45 expression 24 hours after treatment with Sulindac sulfide by real time PCR. Interference with MDA-7/IL-24 expression almost completely blocked Sulindac sulfide-mediated induction of GADD45α and γ gene expression without affecting GADD45β expression (see Fig. 4C in the manuscript Zerbini *et al.* Cancer Research 66: 11922-31, 2006 in the appendices section). These data most vividly demonstrate that GADD45α and γ induction by Sulindac sulfide is mediated via MDA-7/IL-24 upregulation.

MDA-7/IL-24-dependent GADD45α and γ induction and JNK activation are critical for NSAID-mediated apoptosis induction in cancer cells. JNK activation by Sulindac sulfide was at least partially dependent on MDA-7/IL-24 induction, since JNK activity in Sulindac sulfide treated MDA-7/IL-24-/- cells was reduced by 62%, but not completely abolished when compared to MDA-7/IL-24+/+ cells (see Fig. 6C in the manuscript Zerbini *et al*. Cancer Research 66: 11922-31, 2006 in the appendices section).

Aim 3. Determine whether inhibition of the NF-κB pathway enhances Sulindac induced CaP apoptosis (18-36).

We have shown that blockage of the NF-κB pathway leads to apoptosis induction in CaP cells. In our preliminary data, we have shown that overexpression of IκBα induces GADD45α and γ gene expression and activates JNK kinase (1,2). Similarly, Sulindac induces apoptosis in CaP cells and induces GADD45 expression and activates JNK (3). Nevertheless, Sulindac treatment apparently does not inhibit NF-κB and indeed enhances expression of NF-κB dependent genes such as IL-6 and IL-8 rather than inhibiting it. Since activated NF-κB suppresses apoptosis and Sulindac induces apoptosis without inhibiting activated NF-κB, we hypothesize that inhibition of NF-κB in combination with Sulindac should further enhance the pro-apoptotic effect of Sulindac. Various inhibitors of the NF-κB pathway are in preclinical or clinical trials at the moment. Since cancers are very heterogeneous and escape therapy due to resistance via several mechanisms, a two-pronged approach should be significantly more effective in overcoming resistance. The combined interference with NF-κB and the pathways regulated by Sulindac may give rise to novel therapeutic modalities in the fight against various types of cancer. Therefore, we will test the hypothesis that a combination of Sulindac sulfide with an inhibitor of NF-κB will lead to synergistic induction of apoptosis in cancer cells. This combination therapy will be the starting point for a systematic analysis of the molecular mechanisms involved in the effects of a whole panel of NSAIDs on cancer cells.

a) **Determine whether combining Sulindac with NF-κB inhibition enhances apoptosis induction in CaP cells** (Months 18-36)A broad panel of pharmacological inhibitors of the NF-κB pathway was tested for their abilities to induce apoptosis in prostate cancer cells. Apoptosis was measured 24 hours after treatment of DUCaP, VCaP and DU145 prostate cancer cells with this set of inhibitors of the NF-κB, revealing two potent inducers of apoptosis in prostate cancer cells cells. Strong inducers of apoptosis included 6-Amino-4-(4-phenoxyphenylethylamino) quinazoline and IKK-2 inhibitor SC-514 when compared with the solvent controls, whereas treatment with Isohelenin IKK inhibitor II

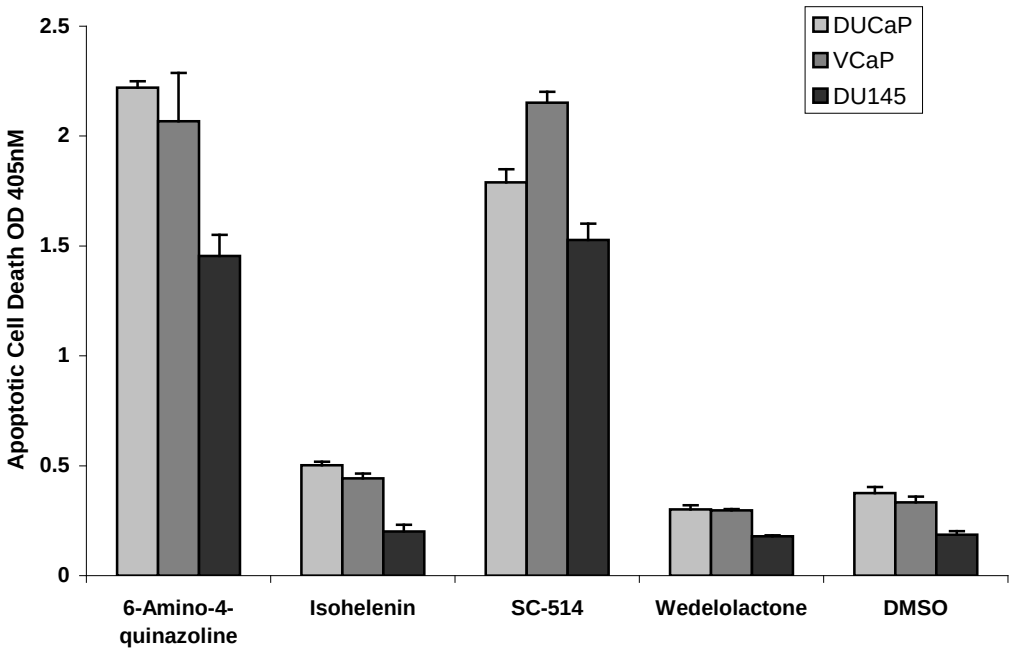

Figure 1. Pharmacological inhibitors of NF-κB induce apoptosis in VCaP and DUCaP and DU145 cells. Cells were treated with 6-Amino-4-(4-phenoxyphenylethylamino)quinazoline, Isohelenin, IKK-2 inhibitor SC-514 and IKK inhibitor II Wedelolactone (7-Methoxy-5,11,12-trihydroxy-coumestan) using DMSO as control. Apoptosis was detected 24 hours post-treatment using the cell death ELISA say (Roche) according to the protocol supplied by the manufacturer.

Wedelolactone (7-Methoxy-5,11,12-trihydroxy-coumestan) resulted only in marginal apoptosis induction (Figure 1).

We extended our studies and determined the lowest dose of the stronger inducers, which still would have an effect in the programmed cell death of prostate cancer cells. Here, we determined the lowest concentrations of NSAIDs and pharmacological inhibitors of NF-κB. The concentrations of pharmacological inhibitors were chosen 2, 5 and 10 times lower than doses used in the experiments mentioned above. The concentrations of selected NSAIDs were also chosen 2, 5 and 10 times lower than doses described in our first annual report and is also described in details in our attached publication (see Figure 1 attached manuscript) . Apoptosis was measured in prostate cancer cells 24 hours after treatment with different doses of NSAIDs and pharmacological inhibitors of NF-κB. Our results showed that the dose of Sulindac Sulfide can be reduced down 10 times, Flufenamic Acid and NS-398 can be reduced down 5 times whereas Finasteride, Diclofenac and Sulindac Sulfone can be reduced 2 times when compared with the solvent controls, and

still resulting in apoptosis induction (Figure 2). Regarding the pharmacological inhibitors of NF-κB, 6-Amino-4-(4-phenoxyphenylethylamino)quinazoline can be reduced 5 times whereas the IKK-2 inhibitor SC-514 can be reduced 2 times when compared with the solvent controls (Figure 2).

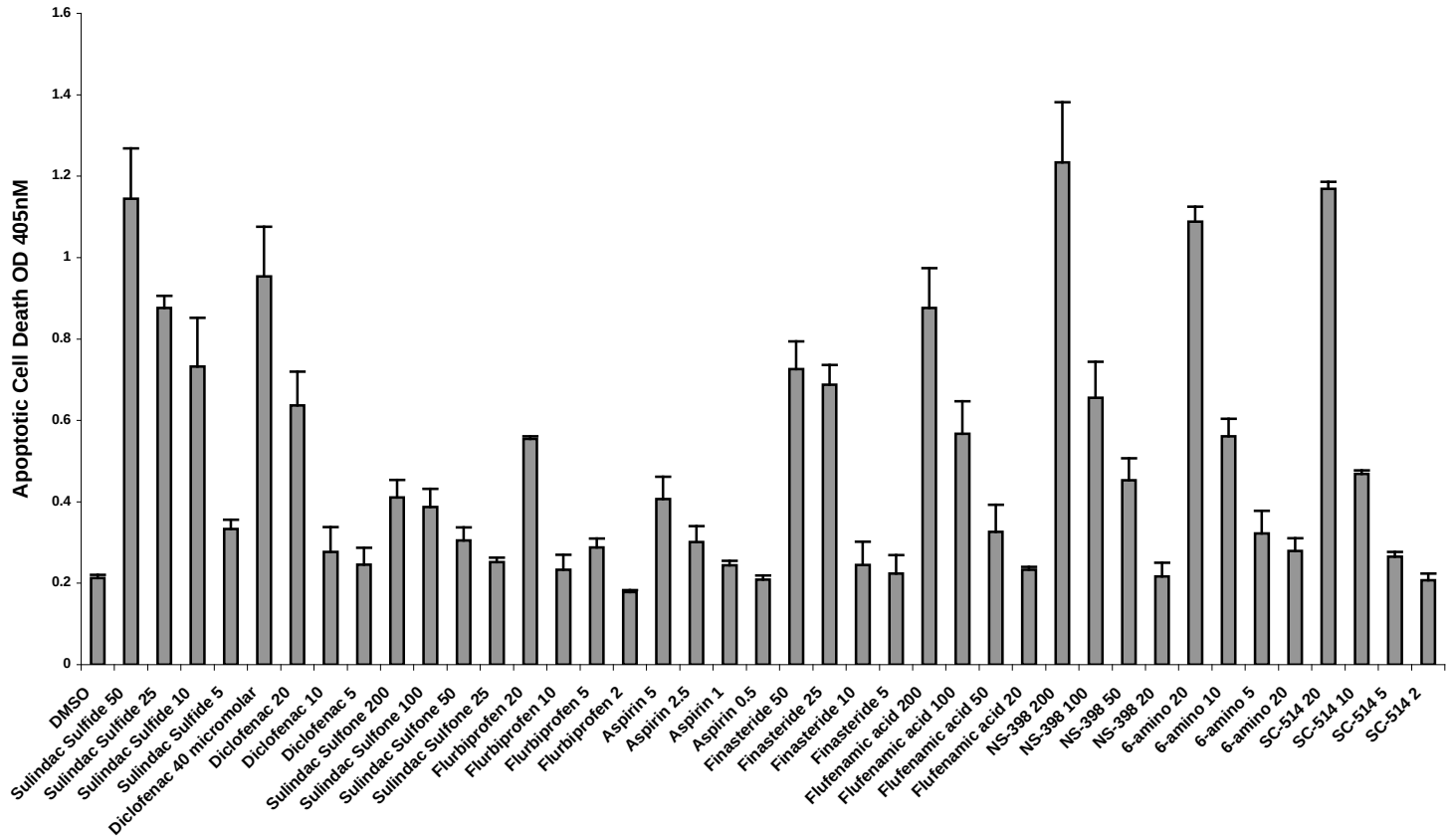

Figure 2. Multiple NSAIDs and pharmacological inhibitors of NF-κB induce apoptosis in prostate cancern cancer cells. Apoptosis assay of DU145 prostate cancer cells. The cells were treated with 50, 25,10 and 5 μM Flufenamic acid and Sulindac Sulfide; 20, 10, 5 and 2nM Flurbiprofen; 50, 25,10 and 5 μM Finasteride; 200, 100,50 and 25 μM NS-398 and Sulindac sulfone; 5, 2.5,1 and 0.5 mM Aspirin, 20, 10, 5 and 2nM 6-Amino-4-(4-phenoxyphenylethylamino)quinazoline, 20, 10, 5 and 2 μM IKK-2 inhibitor SC-514 or DMSO and apoptosis were measured 24 hrs post-treatment. Data means ± s.d. of triplicate independent experiments for each treatment.

Additionally, using the lowest dose of each NSAIDs and pharmacological inhibitors of NF-κB (see Figure 2), we have started to systematically analyze the apoptosis induction of a combination of NSAIDs and NF-κB inhibitors in prostate cancer cells. A panel of NSAIDs including Flufenamic acid, Flurbiprofen, Diclofenac, Sulindac Sulfide, Finasteride and NS398 and NF-B inhibitors 6-Amino-4-(4-phenoxyphenylethylamino) quinazoline and IKK-2 inhibitor SC-514 were tested for their abilities to induce apoptosis alone and in combination thereof. The concentrations used here were the ones defined in Aim 3 as the lowest concentration able to induce apoptosis in prostate cancer cells. DU145 prostate cancer cells were treated with 5μM Flufenamic acid, 5μM Sulindac Sulfide, 50μM NS-398, 5nM Flurbiprofen, 20μM Diclofenac, 25μM Finasteride or 5nM 6-Amino-4-(4-phenoxyphenylethylamino) quinazoline, 10μM IKK-2 inhibitor SC-514 and a combination of them. Apoptosis was measured 24 hours after treatment revealing that the majority of the combination of NSAIDs and pharmacological inhibitors of NF-κB tested, induced apoptosis in prostate cancer cells. However, some combinations had a stinking effect in the apoptosis induction. Strong inducers included Sulindac sulfide+Diclofenac and Sulindac Sulfide+6-Amino-4-(4-phenoxyphenylethylamino) quinazoline(Figure 3).

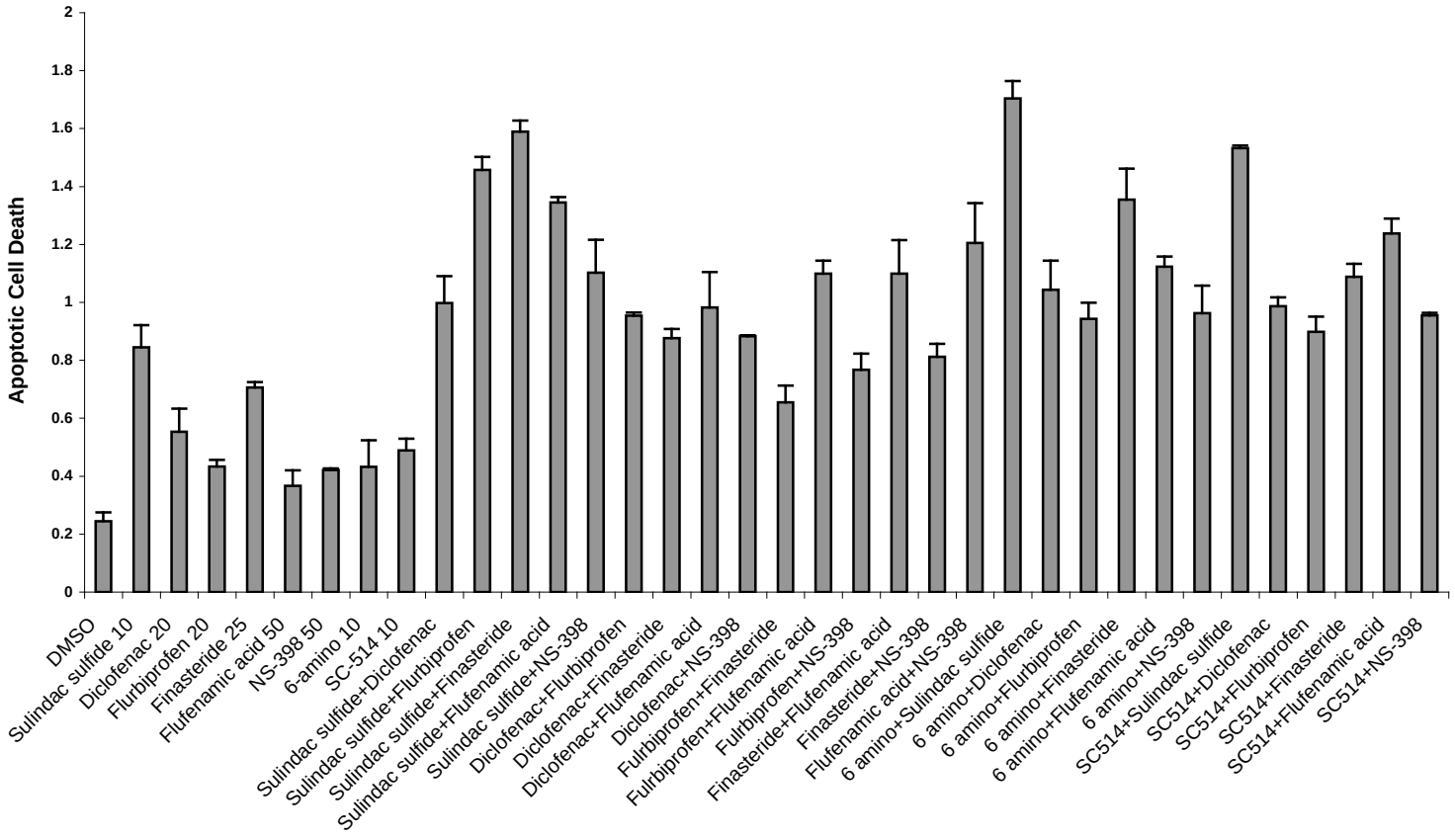

Figure 3. Multiple NSAIDs and pharmacological inhibitors of NF-κB induce apoptosis in quiescent ovarian cancer cells. DU145 prostate cancer cells were treated with 5μM Flufenamic acid, 5μM Sulindac Sulfide, 50μM NS-398, 5nM Flurbiprofen, 20μM Diclofenac, 25μM Finasteride or 5nM 6-Amino-4-(4-phenoxyphenylethylamino) quinazoline, 10μM IKK-2 inhibitor SC-514 and a combination of them or DMSO. Apoptosis was measured 24 hrs post-treatment. Data means ± s.d. of triplicate independent experiments for each treatment.

b) **Determine whether the combination of Sulindac treatment and the blockage of the NF-κB pathway is more effective in inhibiting tumor formation or killing established CaP tumors in SCID mice or TRAMP mice than mono-therapy -** (Months 18-36)

To test whether the blockage of NF-κB in combination with Sulindac treatment is more effective *in vivo*, than either alone we will use the orthotopic tumor model in SCID mice as in our preliminary results and in the attached manuscript. as well as the transgenic adenocarcinoma of the mouse prostate (TRAMP) model (4). Since IκB overexpression itself completely inhibits tumor formation at least in the CaP cell line (1), it is possible that Sulindac sulfide or the pharmacological NF-κB inhibitors inhibit tumor formation as well. tumor size, histopathology, metastases etc. Results from these experiments will most vividly demonstrate whether Sulindac in combination with pharmacological NF-κB inhibitors can efficiently prevent CaP tumor formation or treat established tumors.

We first decided evaluate the toxicity of the chosen inhibitor of NF-κB 6-Amino-4-(4-phenoxyphenylethylamino) quinazoline. This compound was chosen based on our in vitro data (Figure 1 and 2 of this report) which shows the compound as one the stronger inducers of apoptosis in prostate cancer cells as well in combination with NSAIDs.

This first evaluation showed us the drugs develops adverse side effects if administer via IP injection. We then performed experiments using pumps, which releases the drugs in small concentration during 24 hours and added the drugs directly to the diets. Although the use of pumps for drug delivery eliminated the side effects, the combination therapy using NF-κB inhibitor and Sulindac did not show to be more effective than Sulindac treatment alone or statistically significant (data not shown). We also evaluate the tumor formation when the drug was added directly to the diet. However, the results were not different than those described for the use of mini pumps. We also evaluated one more NF-κB inhibitor (SC-514) based on our in vitro data (Figure 1 and 2 of this report). We first evaluate its toxicity and then proceed to animal experiments. Although SC-514 compound did not show side effects as observed with 6-Amino-4-(4-phenoxyphenylethylamino) quinazoline, again the combinatorial therapy with Sulindac did not show to be more effective than the NSAIDS monotherapy. As the NF-κB inhibitors did not prove themselves promising in inhibiting tumor formation in vivo or more effective than Sulindac treatment alone, we decided not move to experiments using TRAMP mouse model. We keep performing screening new NF-κB inhibitors for induction of apoptosis in prostate cancer cells but up to now, I have been unable to find a new compound with strong activity in CaP cells.

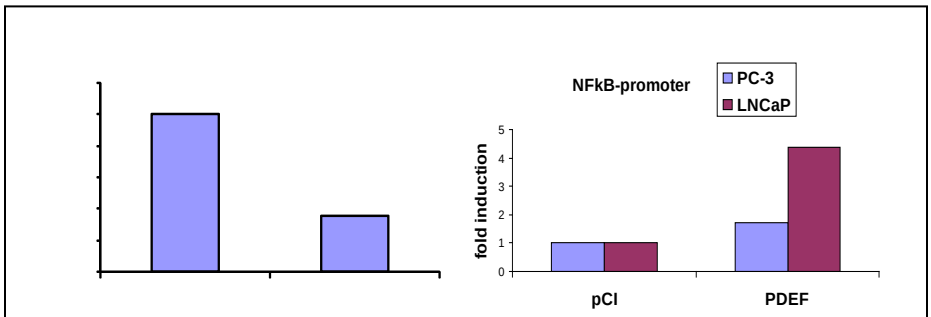

Figure **4. PDEF represses NF-κB activity in prostate cancer cell lines**. A) Repression of PDEF expression using a lentivirus encoding siRNA againt PDEF represses NF-κB activity. B) Overexpression of of PDEF using a adenovirus encoding PDEF gene induces NF-κB activity

During the period of this study, our group collaborated with Dr. Towia Libermann at Beth Israel Deaconess Medical Center in order to develop new approaches for prostate cancer treatment.In one of studies, we identified the epithelium-specific Ets transcription factor, PDEF, as having a important role in prostate. In prostate cancer PDEF is involved in regulating

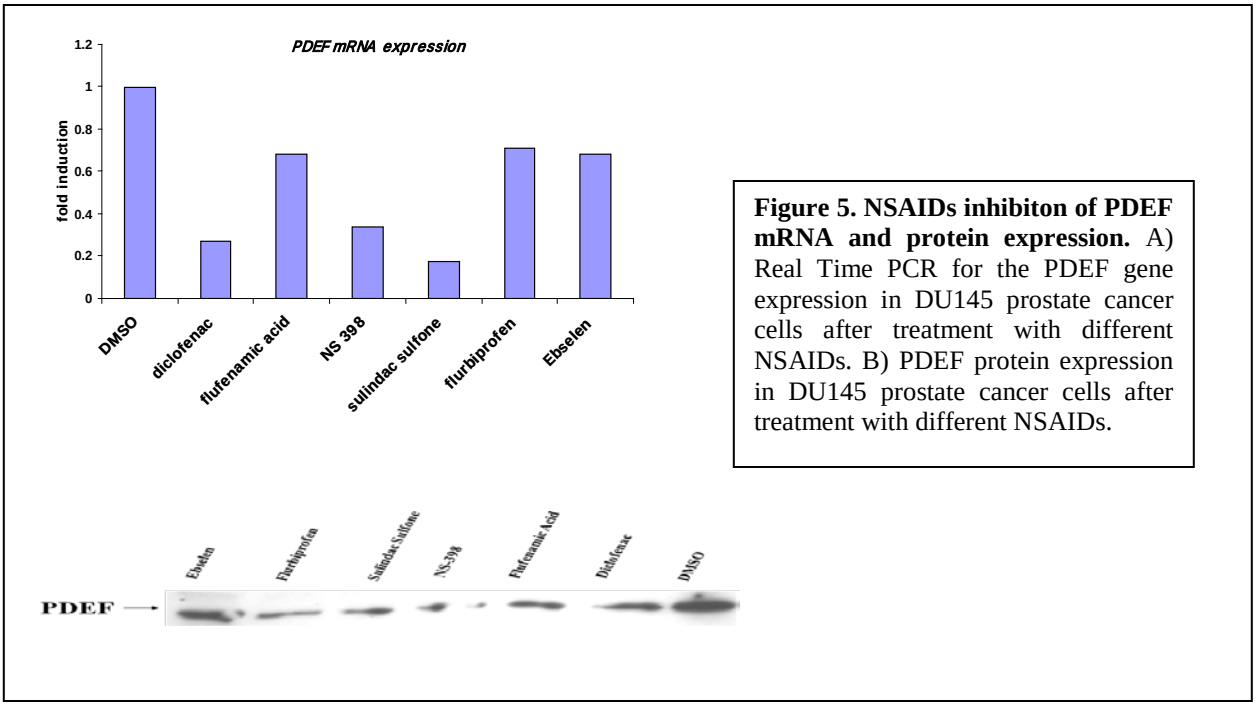

Figure 5. NSAIDs inhibiton of PDEF mRNA and protein expression. A) Real Time PCR for the PDEF gene expression in DU145 prostate cancer cells after treatment with different NSAIDs. B) PDEF protein expression in DU145 prostate cancer cells after treatment with different NSAIDs.

PSA expression via interaction with the androgen receptor and NKX3.1, and downregulation of PDEF by antiproliferative agents has been associated with reduced PDEF expression. We demonstrated thatreduced expression of PDEF leads to a morphological change, increased migration and invasiveness in prostate cancer cells, reminiscent of TGFβ function and EMT (epithelial-to-mesenchymal transition). Indeed, inhibition of PDEF expression triggers a transcriptional program of genes involved in the TGFβ pathway, migration, invasion, adhesion, andepithelial dedifferentiation. Our results establish PDEF as a critical regulator of genes involved in cell motility, invasion and adhesion of prostate cancer cells (see attached manuscript Gu *et al*. Cancer Research 67: 4219-26, 2007).

We further test whether PDEF could have an effect in NF-κB activation. As seen in figure 4A, inhibition of PDEF using siRNA technology, inhibits NF-κB activation and overexpression of PDEF using an adenovirus encoding PDEF enhances NF-κB activity in prostate cancer cells (Figure 4B). Additionally, we evaluated whether PDEF plays a role during NSAIDs-mediated apoptosis in prostate cancer. We measured mRNA expression and protein levels of PDEF in response to different NSAIDS treatment in the prostate cancer cell lines. Real time PCR and western blot analysis demonstrated that NSAIDs represses PDEF expression (Figures 5A and B). These results indicates that NSAIDs mediated repression of PDEF expression strongly suggest that PDEFplays a critical role in apoptosis induction. We are testing now what are the molecular mechanisms of PDEF regulation of NF-κB target genes with particular focus on MDA-7/IL-24 and the GADD45 family of genes.

Key Research Accomplishments

- We report the discovery of a novel biological pathway involving MDA-7/IL-24 and the GADD45 gene family that are targeted by a set of NSAIDs in prostate cancer and whose activation directly correlates with the efficacy of NSAIDs to induce cancer cell death.
- We demonstrate that multiple classes of structurally unrelated NSAIDs induce apoptosis and growth arrest via induction of MDA-7/IL-24 expression that leads to GADD45α and γ expression and JNK activation and G2/M cell cycle arrest due to GADD45α and γ dependent inhibition of Cdc2 activity.
- Our discovery of specific high level induction of MDA-7/IL-24 in different types of cancer cells including prostate cancer by a variety of NSAIDs provides a new entry point to enhance MDA-7/IL-24 levels in cancer cells on a systemic level.
- Our in vivo orthotopic tumor model further supports the notion that MDA-7/IL-24 is indeed a tumor suppressor gene. It also suggests that MDA-24/IL24 is not the unique pathway targeted.
- Our data provide strong evidence that multiple NSAIDs induce cancer cell death through MDA-7/IL-24-mediated upregulation of GADD45α and γ, irrespective of their ability to block COX-2. For example, Finasteride, a selective 5-alpha-reductase inhibitor, is not known to inhibit COX-2, strongly induces MDA-7/IL-24 expression and apoptosis, whereas the potent selective COX-2 inhibitor Celecoxib is significantly less effective in inducing MDA-7/IL-24 and apoptosis. On the other hand, the non-selective cation channel blocker flufenamic acid and the non-selective COX-1 and COX-2 inhibitors Sulindac sulfide and Diclofenac are very potent inducers of MDA-7/IL-24 and apoptosis. Thus, the pro-apoptotic anti-cancer activity of several divergent classes of drugs evaluated here appears not to be due to their effects on their supposed targets, but due to the off-target induction of MDA-7/IL-24.
- We have successfully defined the strong pharmacological inhibitors of NF-κB inducers of apoptosis in prostate cancer cells lines

- We have successfully determined the lowest dose of NSAIDs and pharmacological inhibitors of NF-κB described above for induction of apoptosis in prostate cancer cells lines
- We also have successfully determined the best NSAIDs combination and NSAIDs and pharmacological inhibitors of NF-κB for induction of apoptosis in prostatecancer cells lines
- We also have successfully determined a new player in the apoptosis induction by NSAIDs. PDEF transcription factor has a direct effect in NF-κ activation and is repressed by NSAIDs.

Reportable Outcomes

Zerbini LF, Czibere A, Wang Y, Correa RG, Out H, Joseph M, Takayasu Y, Silver M, Gu X, Li L, Sarkar D, Zhou JR, Fisher PB and Libermann TA. A novel pathway involving MDA-7/IL-24 mediates NSAID induced apoptosis of cancer cells. **Cancer Research** 66: 11922-31. 2006.

Gu X, Zerbini LF, Otu H, Joseph MG, Grall F, Correa RG, Libermann TA Reduced PDEF expression leads to an increase in cell motility, invasion and expression of mesenchymal genes in prostate cancer cells. **Cancer Research** 67: 4219-4226. 2007

Conclusion

The ability of NSAIDs to induce apoptosis appears to depend on their abilities to induce MDA-7/IL-24 expression and enhance GADD45α and γ expression. Thus, apoptosis and growth arrest induction of cancer cells as a result of enhanced MDA-7/IL-24 expression appears to be a common pathway for multiple classes of drugs. Pharmacological inhibitors of NF-κB have a potent effect in apoptosis induction of prostate cancer cells as well as in combination with NSAIDs

These results also provide a rationale to screen small molecule libraries, natural compound libraries and chemically modified NSAIDs for selective inducers of MDA-7/IL-24 expression in cancer cells in order to obtain more effective anti-cancer drugs. These new compounds could be then tested in combination of inhibitors of NF-κB pathway which are already in clinical trials.

References

(1) Zerbini LF, Czibere A, Wang Y, Correa RG, Out H, Joseph M, Takayasu Y, Silver M, Gu X, Li L, Sarkar D, Zhou JR, Fisher PB and Libermann TA. A novel pathway involving MDA-7/IL-24 mediates NSAID induced apoptosis of cancer cells. Cancer Research 2006; 66: 11922-31.

(2) Ravis WR, Diskin CJ, Campagna KD, Clark CR, McMillian CL. Pharmacokinetics and dialyzability of sulindac and metabolites in patients with end-stage renal failure. J Clin Pharmacol 1993; 33:527-34..

(3) Swanson BN, Boppana VK, Vlasses PH, Holmes GI, Monsell K, Ferguson RK. Sulindac disposition when given once and twice daily. Clin Pharmacol Ther 1982;32:397-403.

(4) Davies NM, Watson MS. Clinical pharmacokinetics of sulindac. A dynamic old drug. Clin Pharmacokinet 1997;32:437-59

(5) Mita, H, Tsutsui, J, Takekawa, M, Witten, EA, and Saito, H. Regulation of MTK1/MEKK4 kinase activity by its N-terminal autoinhibitory domain and GADD45 binding. Mol Cell Biol 2002; 22:4544-4555..

(6) Jin, S, Antinore, MJ, Lung, FD, *et al.* The GADD45 inhibition of Cdc2 kinase correlates with GADD45-mediated growth suppression. J Biol Chem 2000; 275:16602-16608.
(7) Vairapandi, M, Balliet, AG, Hoffman, B, and Liebermann, DA. GADD45b and GADD45g are cdc2/cyclinB1 kinase inhibitors with a role in S and G2/M cell cycle checkpoints induced by genotoxic stress. J Cell Physiol 2002; 192:327-338.
(8) Wang, XW, Zhan, Q, Coursen, JD, *et al.* GADD45 induction of a G2/M cell cycle checkpoint. Proc Natl Acad Sci U S A 1999; 96:3706-3711.
(9) Jiang, H, Lin, JJ, Su, Z-z, Goldstein, NI, and Fisher, PB. Subtraction hybridization identifies a novel melanoma differentiation associated gene, mda-7, modulated during human melanoma differentiation, growth and progression. Oncogene 1995; 11:2477-2486.
(10) Fisher, PB. Is mda-7/IL-24 a "magic bullet" for cancer? Cancer Res. 2005; 65:10128-10138.
(11) Gupta, P, Su, Z-z., Lebedeva, IV, *et al.* mda-7/IL-24: Multifunctional cancer-specific apoptosis-inducing cytokine. Pharmacol. & Therap. 2006; 11:596-628.
(12) Su, Z-z, Lebedeva, IV, Sarkar, D, *et al.* Melanoma differentiation associated gene-7, mda-7/IL-24, selectively induces growth suppression, apoptosis and radiosensitization in malignant gliomas in a p53-independent manner. Oncogene 2003; 22:1164-1180.
(13) Ishikawa, S, Nakagawa, T, Miyahara, R, *et al.* Expression of MDA-7/IL-24 and its clinical significance in resected non-small cell lung cancer. Clin Cancer Res 2005; 11:1198-1202.
(14) Zerbini, LF, Wang, Y, Czibere, A, *et al.* NF-kappa B-mediated repression of growth arrest- and DNA-damage-inducible proteins 45alpha and gamma is essential for cancer cell survival. Proc Natl Acad Sci U S A 2004; 101:13618-13623.
(15) Sarkar, D, Su, ZZ, Lebedeva, IV, *et al.* mda-7 (IL-24) Mediates selective apoptosis in human melanoma cells by inducing the coordinated overexpression of the GADD family of genes by means of p38 MAPK. Proc Natl Acad Sci U S A 2002; 99:10054-10059.

Appendices

See attached manuscripts

A Novel Pathway Involving Melanoma Differentiation Associated Gene-7/Interleukin-24 Mediates Nonsteroidal Anti-inflammatory Drug–Induced Apoptosis and Growth Arrest of Cancer Cells

Luiz F. Zerbini,[1] Akos Czibere,[1] Yihong Wang,[1] Ricardo G. Correa,[3] Hasan Otu,[1] Marie Joseph,[1] Yuko Takayasu,[1] Moriah Silver,[1] Xuesong Gu,[1] Kriangsak Ruchusatsawat,[1] Linglin Li,[2] Devanand Sarkar,[4] Jin-Rong Zhou,[2] Paul B. Fisher,[4] and Towia A. Libermann[1]

[1]BIDMC Genomics Center and [2]Department of Surgery, Beth Israel Deaconess Medical Center and Harvard Medical School, Boston, Massachusetts; [3]Laboratory of Genetics, The Salk Institute for Biological Studies, La Jolla, California; and [4]Departments of Pathology and Urology, Columbia University Medical Center, College of Physicians and Surgeons, New York, New York

Abstract

Numerous studies show that nonsteroidal anti-inflammatory drugs (NSAIDs) are effective in chemoprevention or treatment of cancer. Nevertheless, the mechanisms underlying these antineoplastic effects remain poorly understood. Here, we report that induction of the cancer-specific proapoptotic cytokine melanoma differentiation associated gene-7/interleukin-24 (*MDA-7/IL-24*) by several NSAIDs is an essential step for induction of apoptosis and G_2-M growth arrest in cancer cells *in vitro* and inhibition of tumor growth *in vivo*. We also show that MDA-7/IL-24–dependent up-regulation of *growth arrest and DNA damage inducible 45 α* (*GADD45α*) and *GADD45γ* gene expression is sufficient for cancer cell apoptosis via c-Jun NH_2-terminal kinase (JNK) activation and growth arrest induction through inhibition of Cdc2-cyclin B checkpoint kinase. Knockdown of *GADD45α* and *GADD45γ* transcription by small interfering RNA abrogates apoptosis and growth arrest induction by the NSAID treatment, blocks JNK activation, and restores Cdc2-cyclin B kinase activity. Our results establish MDA-7/IL-24 and GADD45α and GADD45γ as critical mediators of apoptosis and growth arrest in response to NSAIDs in cancer cells. (Cancer Res 2006; 66(24): 11922-31)

Introduction

Various studies indicate that nonsteroidal anti-inflammatory drugs (NSAIDs), at clinically relevant concentrations, may be effective in prevention and treatment of common cancers (1, 2). Epidemiologic studies have suggested that regular use of certain NSAIDs reduces the risk of colorectal, breast, and ovarian cancer, and the number of precancerous colorectal polyps (3–5). The detailed molecular mechanisms by which NSAIDs inhibit neoplastic growth are, however, poorly understood and likely involve many off-target and divergent activities among different NSAIDs. Additionally, current clinical trials are evaluating a range of NSAIDs for a variety of cancers without any clear vision of the best way to use them.

Preclinical efficacy studies in animal models and cancer cell lines show strong antineoplastic effects of NSAIDs *in vivo* and *in vitro* (6, 7). The chemopreventive and antitumorigenic effects of NSAIDs are, to a large part, attributed to their apoptosis-inducing potential and may involve cyclooxygenase-2 (COX-2) inhibition (8–11). Nevertheless, the relevance of COX-2 inhibition for apoptosis induction is not entirely clear, because apoptosis induction by NSAIDs does not always correlate with their abilities to inhibit COX-2. Chemical modifications of NSAIDs that select for NSAIDs with enhanced proapoptotic activity reveal that structural requirements necessary for inhibition of cell growth and apoptosis induction in cancer cells can be distinct from those effecting COX-2 inhibition (12–15).

Because COX-2 inhibition does not seem to be the only antineoplastic, proapoptotic pathway targeted by NSAIDs in cancer cells, it is essential to unravel the molecular processes involved in apoptosis induction by these agents (16–18). Understanding these mechanisms will help to design drugs that are more specifically targeted against cancer, and, indeed, recent efforts show that chemical modifications of NSAIDs enable the selection of more efficient inducers of cancer cell apoptosis with enhanced growth inhibitory properties.

The objectives of our study were to obtain a comprehensive view of NSAID-mediated apoptosis in cancer cells and to decipher the precise molecular mechanisms of action by surveying and comparing a complete set of NSAIDs for their efficacies to induce apoptosis and growth arrest in cancer cells. We describe here a novel pathway by which NSAIDs induce apoptosis and growth arrest in cancer cells. We show that induction of the proapoptotic cytokine melanoma differentiation associated gene-7/interleukin-24 (*MDA-7/IL-24*) that mediates induction of growth arrest and DNA damage inducible 45 α (*GADD45α*) and *GADD45γ* expression (18–21) is sufficient for NSAID-induced cancer cell apoptosis and growth arrest. MDA-7/IL-24 overexpression is currently used in clinical trials, and identification of drugs that are most efficient in MDA-7/IL-24 induction may significantly enhance the antineoplastic effect of this novel cytokine.

Materials and Methods

Cell culture. The prostate cancer cell lines LNCaP, DU145, and PC-3; renal cancer cell lines Caki, UOK, A704, ACHN, and A498; stomach cancer cell lines Kato, SNU1, SNU16, NCI, and AGS1; breast cancer cell lines MDA231, MDA453, MDA435, SKBR3, and MCF-7; and the HEK 293 cell line

---

Note: Supplementary data for this article are available at Cancer Research Online (http://cancerres.aacrjournals.org/).

L.F. Zerbini and A. Czibere contributed equally to this work. K. Ruchusatsawat is a fellow of the Royal Golden Jubilee grant, Thailand Research Funds.

Current address for A. Czibere: Department of Haematology, Oncology, and Clinical Immunology, Heinrich Heine-University, Düsseldorf, Germany.

Current address for R.G. Correa: Department of Biochemistry, Institute of Chemistry, University of São Paulo, São Paulo, Brazil.

Requests for reprints: Towia A. Libermann, BIDMC Genomics Center and Dana-Farber/Harvard Cancer Center Cancer Proteomics Core, Beth Israel Deaconess Medical Center and Harvard Medical School, Harvard Institutes of Medicine, 4 Blackfan Circle, Boston, MA 02115. Phone: 617-667-3393; Fax: 617-975-5299; E-mail: tliberma@bidmc.harvard.edu.

doi:10.1158/0008-5472.CAN-06-2068

were obtained from American Type Culture Collection (Rockville, MD). The F-12 foreskin fibroblast cell line was kindly provided by Dr. Steven Goldring (Beth Israel Deaconess Medical Center), and the CW19 and CW22 prostate cancer cell lines were kindly provided by Dr. Steven P. Balk (Beth Israel Deaconess Medical Center). The MS-1 endothelial cell line was kindly provided by Peter Oettgen (Beth Israel Deaconess Medical Center). A704, ACHN A498, and DU145 cells were grown in MEM (Life Technologies, Carlsbad, CA); CW19, CW22, MDA231, MCF-7, SKBR3, MDA453, MDA435, UOK, MS-1, F-12, and HEK 293 were grown in DMEM (Life Technologies); LNCaP, SNU1, SNU16, Kato, and NCI were grown in RPMI medium (Life Technologies); Caki cells were grown in McCoy's 5A medium (Life Technologies); and AGS1 and PC-3 cells were grown in HAMS F-12 medium (BioWhitaker, Walkersville, MD). The medium was supplemented with 10% fetal bovine serum (FBS), 50 units penicillin/mL, and 50 μg streptomycin/mL (all from Life Technologies). The cells were maintained in a 5% CO_2–humidified incubator at 37°C.

Reagents. Sulindac sulfide, sulindac sulfone, ibuprofen, aspirin, acetaminophen, and naproxen were obtained from Sigma-Aldrich (St. Louis, MO). Meloxicam, celecoxib, diclofenac, finasteride, and flufenamic acid were obtained from LKT Laboratories (St. Paul, MN). NS-398, ebselen, and flurbiprofen were purchased from Calbiochem (San Diego, CA). The drugs were dissolved in DMSO or ethanol. Cancer cells were treated in their particular medium for 24 hours. The final concentration for each compound were as follows: 50 μmol/L sulindac sulfide, 5 mmol/L aspirin, 200 μmol/L ibuprofen, 50 μmol/L sulindac sulfone, 1 mmol/L acetaminophen, 200 μmol/L naproxen, 200 μmol/L NS-398, 50 μmol/L celecoxib, 40 μmol/L diclofenac, 50 μmol/L finasteride, 200 μmol/L flufenamic acid, 10 μmol/L meloxicam, 50 μmol/L ebselen, and 20 nmol/L flurbiprofen. For the controls, cells were treated with an equal amount of DMSO or ethanol, which was <0.1% of the final concentration.

Real-time PCR. Total RNA was harvested using QIAshredder (Qiagen, Valencia, CA) and RNeasy Mini kit (Qiagen). Real-time PCR was done as described (20). cDNAs were generated from 2 μg of total RNA using Ready-to-Go You-Prime First-Strand Beads (Amersham Pharmacia Biotech, Inc., Piscataway, NJ). Amplifications of 0.1 μg cDNA were carried out using SYBR Green I–based real-time PCR on the MJ Research DNA Engine Opticon Continuous Fluorescence Detection System (MJ Research, Inc., Waltham, MA). All PCR mixtures contained PCR buffer [final concentration 10 mmol/L Tris-HCl (pH 9.0), 50 mmol/L KCl, 2 mmol/L $MgCl_2$, and 0.1% Triton X-100], 250 μmol/L deoxynucleotide triphosphate (Roche, Indianapolis, IN), 0.5 μmol/L of each PCR primer, 0.5× SYBR Green I (Molecular Probes, Eugene, OR), 5% DMSO, and 1 unit Taq DNA polymerase (Promega, Madison, WI) with 2 μL cDNA in a 25 μL final volume reaction mix. The samples were loaded into wells of low-profile, 96-well microplates. After an initial denaturation step of 60 seconds at 94°C, conditions for cycling were 40 cycles of 30 seconds at 94°C, 30 seconds at 52°C, and 1 minute at 72°C. Then, the fluorescence signal was measured right after incubation for 5 seconds at 79°C that follows the extension step, which eliminates possible primer dimer detection. At the end of the PCR cycles, a melting curve was generated to identify the specificity of the PCR product. For each run, serial dilutions of human glyceraldehyde-3-phosphate dehydrogenase (hGAPDH) plasmids were used as standards for quantitative measurement of the amount of amplified DNA. Also, for normalization of each sample, hGAPDH primers were used to measure the amount of hGAPDH cDNA. All samples were run in triplicates and the data were presented as gene-to-GAPDH ratio. The sequences of the primers are as follows: for *GADD45α*, sense 5′-GCC-TGTGAGTGAGTGCAGAA-3′; antisense 5′-ATCTCTGTCGTCGTCCTCGT-3′; for *GADD45β*, sense 5′-TCGGATTTTGCAATTTCTCC-3′; antisense 5′-GGAT-GAGCGTGAAGTGGATT-3′; for *GADD45γ*, sense 5′-CTGCATGAGTTGCTG-CTGTC-3′; antisense 5′-TTCGAAATGAGGATGCAGTG -3′; for *MDA-7/IL-24*, sense 5′-CAAAGCCTGTGGACTTTAGCC-3′; antisense 5′-GAATAGCAGAAA-CCGCCTGTG-3′; and for *hGAPDH*, sense 5′-CAAAGTTGTCATGGATGACC-3′; antisense 5′-CCATGGAGAAGGCTGGGG-3′.

Western blot analysis. Whole-cell lysates were prepared in lysis buffer [20 mmol/L Tris (pH 7.4), 150 mmol/L NaCl, 1 mmol/L EDTA, 1 mmol/L EGTA, 1% Triton X-100, 2.5 mmol/L sodium PPi, 1 mmol/L β-glycerolphosphate, 1 mmol/L Na_3VO_4, 1 μg/mL leupeptin, and 1 mmol/L phenylmethylsulfonyl fluoride] of treated and control cells. One hundred micrograms of protein were electrophoresed in a 10% SDS-polyacrylamide gel. Proteins were electroblotted onto polyvinylidene difluoride membranes in a 50 mmol/L Tris base, 20% methanol, and 40 mmol/L glycine electrophoresis buffer. Membranes were incubated in 5% nonfat dry milk in TBST (60 mmol/L Tris-base, 120 mmol/L NaCl, 0.2% Tween 20) for 1 hour. Blots were probed with primary antibody overnight at 4°C in 2% bovine serum albumin in TBST, and then incubated with a horseradish peroxidase–conjugated secondary antibody (Cell Signaling Technology, Danvers, MA) in 5% dry milk in TBST for 1 hour at room temperature. Bound antibodies were detected by chemiluminescence with enhanced chemiluminescence detection reagents (Amersham Pharmacia Biotech) and were visualized by autoradiography. The primary antibodies used for Western blot analysis were anti-CDC25C (Cell Signaling Technology), anti-cyclin B1 (EMD Biosciences, San Diego, CA), anti-cyclin B2 (Santa Cruz Biotechnology), anti-phospho c-Jun (Cell Signaling Technology), anti-p21 (Cell Signaling Technology), anti-GADD45α (Santa Cruz Biotechnology), anti-GADD45β (Santa Cruz Biotechnology), and anti-GADD45γ (Santa Cruz Biotechnology). The MDA-7/IL-24 antibody was kindly provided by Sunil Chada (Introgen, Inc.).

Kinase assays. Cdc2 kinase assay was done using histone H1 as the Cdc2 substrate. Five hundred micrograms of the cell lysate were immunoprecipitated using 2 μg agarose-conjugated anti-Cdc2 monoclonal antibody (Santa Cruz Biotechnology) overnight at 4°C. The beads were washed twice with lysis buffer and twice with kinase buffer [25 mmol/L Tris (pH 7.5), 5 mmol/L β-glycerolphosphate, 2 mmol/L DTT, 0.11 mmol/L Na_3VO_4, 10 mmol/L $MgCl_2$] and subjected to the kinase assays. The beads were suspended in 50 μL of kinase buffer supplemented with 200 μmol/L ATP and 30 μL Cdc2 substrate cocktail [Upstate; 2 mg/mL histone H1 in 20 mmol/L MOPS (pH 7.2), 25 mmol/L β-glycerophosphate, 5 mmol/L EGTA, 1 mmol/L sodium orthovanadate, 1 mmol/L DTT], and incubated for 30 minutes at 30°C. The reactions were terminated by adding 25 μL of 3× SDS sample buffer, and proteins were resolved by SDS-10% PAGE and probed with phospho-histone H1 antibody (Upstate). Active Cdc2 directly correlates with enhanced phosphorylation of histone H1. c-Jun NH_2-terminal kinase (JNK) kinase activity was measured by using the stress-activated protein kinase (SAPK)/JNK assay kit (Cell Signaling Technology) according to the manufacturer's protocol and as described in the supporting text.

Apoptotic assays. Apoptosis was assayed by using the Apoptotic Cell Death Detection ELISA (Roche) and/or the Cell Death Detection (Nuclear Matrix Protein, San Diego, CA) ELISA (EMD Biosciences) according to the manufacturer's protocol.

Animals, diets, and orthotopic implantation of DU145 tumor cells. Eight-week-old male severe combined immunodeficient (SCID)-beige mice were purchased from Taconic (Germantown, NY) and housed in a pathogen-free environment. Immediately before implantation, DU145 cells infected with lentiviral vector small interfering RNA green fluorescent protein (LV-siRNA GFP) or LV-siRNA MDA-7/IL-24 or uninfected cells were trypsinized and resuspended in MEM with 10% FBS. Cell viability was determined by trypan blue exclusion. Then, a single cell suspension with >90% viability was used for implantation. A transverse incision was made in the lower abdomen, and the bladder and seminal vesicles were delivered through the incision to expose the dorsal prostate. DU145 cells (2×10^6 in 50 μL) were carefully injected under the prostatic capsule via a 30-gauge needle as described previously (20). Proper inoculation of cell suspension was indicated by blebbing under the prostate capsule. The incision was closed using a running suture of 5-0 silk. All procedures with animals were reviewed and approved by the Institutional Animal Care and Use Committee at the Beth Israel Deaconess Medical Center according to NIH guidelines. The mice were randomly divided into two groups (n = 8 per group) and fed one of two diets through the entire experiment: AIN-93G as the control and the AIN-93G diet supplemented with 200 ppm sulindac sulfide. The diets were prepared by Research Diets, Inc. (New Brunswick, NJ). Body weight and food intake were measured weekly. Six weeks after cancer cell implantation, phlebotomy was done by accessing the retro-orbital venous plexus to obtain 150 μL of blood from each mouse. Serum IL-6 level was measured by ELISA to estimate the tumor-take rate and tumor size. At the end of the experiment (8 weeks), animals were sacrificed

and tumors were carefully dissected and weighed. Lymph nodes and lungs were collected to determine metastases.

siRNA oligonucleotides and transfections. The oligonucleotides for the three GADD45 family members have been described (20). The sense-strand sequence for each siRNA (Dharmacon, Chicago, IL) is described (a complementary oligonucleotide was synthesized for each): MDA-7/IL-24 siRNA 5′-AACTTTGTTCTCATCGTGTCA-3′. RNA duplexes (50 μmol/L) were transfected into cells using TKO transfection reagent (Mirus, Madison, WI) and tested for specificity and efficiency (see Supplementary Fig. S5*C*).

Adenovirus constructs. The adenoviruses encoding *β-galactosidase* (Ad5-CMVβ-gal) and *MDA-7/IL-24* (Ad5-MDA-7/IL-24) genes were described previously (20, 21).

siRNA lentiviral vectors. The lentiviruses encoding siRNA against the three GADD45 family members have been described (20). The LV-siRNA GFP construct (control) was kindly donated by Dr. Oded Singer (Salk Institute for Biological Studies). The lentivirus encoding siRNA against *MDA-7/IL-24* gene was cloned using Advantage 2 PCR kit (Clontech, Mountain View, CA), and the virus was generated by using a previously described methodology (20). The following siRNA oligonucleotides were used: 5′-CTGTCTAGACAAAAACTTTGTTCTCATCGTGTCATCT-CTTGAATGACACGATGAGAACAAAGGGGGATCTGTGGTCTCATACA-3′ for MDA-7/IL-24.

Production of lentiviral vectors and infections. Vesicular stomatitis virus G envelope protein-pseudotyped lentiviruses were prepared and purified as described (20). The specificity of all lentivirus vectors was tested (see supporting text).

Microarray analysis. Total RNA was harvested from cells treated with 50 μmol/L sulindac sulfide or DMSO 24 hours posttreatment using QIAshredder (Qiagen) and RNeasy Mini kit (Qiagen) and converted into cRNA according to manufacturer's instructions (Affymetrix, Santa Clara, CA). Experiments were done in duplicates. cRNAs were hybridized to the HG-U133A gene array (Affymetrix), washed, and scanned according to the manufacturer's instructions (Affymetrix). Scanned array images were analyzed by dChip, where model-based gene expression values were obtained using a smoothing-spline normalization method (22) to compare two groups of samples aiming to identify genes enriched in a given phenotype. If 90% lower confidence bound of the fold change between the two groups was >1.2, the corresponding gene was considered to be differentially expressed (22). Lower confidence bound is a stringent estimate of fold change and has been shown to be the better-ranking statistic (23). It has been suggested that a criterion of selecting genes that have a lower confidence bound above 1.2 most likely corresponds to genes with an "actual" fold change of at least 3 in gene expression (22–24).

Cell cycle analysis. Prostate cancer cells were treated with NSAIDs or DMSO as described above. After 24 hours of treatment, the medium was replaced by serum-containing medium, and cells were allowed to grow for another 24 hours. The cells were trypsinized, washed twice with cold PBS containing 2% FBS, and fixed in 70% ethanol for 60 minutes at 4°C. The cells were then washed twice with PBS and stained with 200 μL propidium iodide stock solution (50 μg/mL propidium iodide, 3.8 mmol/L sodium trisphosphate in PBS) supplemented with 50 μL RNase A (10 μg/mL) for 3 hours at 4°C and then analyzed with a FACScan cell sorter (Becton Dickinson, Franklin Lakes, NJ). Ten thousand cells were collected and the cell cycle profiles were calculated using the Cellquest Software.

Results

Multiple NSAIDs are potent inducers of apoptosis in prostate cancer cells. A broad panel of NSAIDs was tested for their abilities to induce apoptosis in cancer cells. The concentrations for all NSAIDs used in this study were selected to reflect achievable plasma concentrations (25–40). However, some drug concentrations exceeded the physiologically achievable doses (25–40). Apoptosis was measured 24 and 48 hours after treatment of DU145 prostate cancer cells with this set of NSAIDs, revealing that a variety of, but not all, NSAIDs induced apoptosis in DU145 cells. Strong inducers of apoptosis included sulindac sulfide, finasteride, diclofenac, flufenamic acid, flurbiprofen, sulindac sulfone, and NS-398 compared with solvent controls, whereas treatment with aspirin, celecoxib, acetaminophen, ibuprofen, naproxen, meloxicam, and ebselen resulted in only marginal apoptosis induction (Fig. 1). Sulindac sulfide was the strongest inducer of apoptosis in DU145 cells and it was one of the top three apoptotic inducers in a variety of cancer cells (data not shown).

NSAIDs induce G_2-M growth arrest and apoptosis in cancer cells. Sulindac sulfide and sulindac sulfone are the two major metabolites of sulindac sulfoxide (Clinoril; Merck, Whitehouse Station, NJ). Whereas sulindac sulfide is a COX-2 inhibitor, the sulfone compound is considered not to block COX-2. Sulindac sulfide inhibits proliferation and suppresses growth of various types of cancers in xenograft mouse models (refs. 41, 42; Supplementary Fig. S1*A* and *B*). The role of NSAIDs, such as sulindac sulfide, in growth arrest remains less well characterized. Cell cycle analysis of DU145 and PC-3 cells treated with 50 μmol/L sulindac sulfide for 24 hours revealed that sulindac sulfide induced G_2-M growth arrest in both prostate cancer cell lines when compared with control (Supplementary Fig. S2) by increasing the fraction of cells in the G_2-M phase by 2-fold (25–27).

To evaluate whether sulindac sulfide induces apoptosis in cancer cells, prostate, breast, renal, and stomach cancer cell lines, as well as untransformed cells, were treated with sulindac sulfide for 24 hours. Sulindac sulfide induced apoptosis in most prostate cancer cell lines and in almost all breast, renal, and stomach cancer cell lines except the A704 renal cancer cell line (Fig. 2). In contrast, untransformed cells, such as the MS-1 endothelial and F12 foreskin fibroblast cells, were not affected by sulindac sulfide, demonstrating broad-range specificity for cancer cells (Fig. 2). Moreover, a time course experiment showed that sulindac sulfide started to induce programmed cell death as early as 12 hours posttreatment (Supplementary Fig. S3*A*).

It has been established that sulindac sulfide reaches peak plasma concentrations of 30 to 50 μmol/L (25–27), coming down to a steady-state plasma concentration of 5 to 10 μmol/L (43). We,

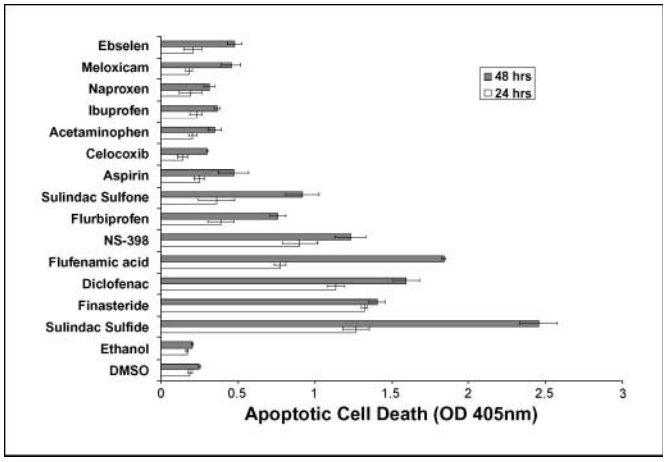

Figure 1. Multiple NSAIDs induce apoptosis in cancer cells. Apoptosis assay of DU145 prostate cancer cells after treatment with 50 μmol/L sulindac sulfide, 5 mmol/L aspirin, 200 μmol/L ibuprofen, 200 μmol/L sulindac sulfone, 1 mmol/L acetaminophen, 200 μmol/L naproxen, 200 μmol/L NS-398, 50 μmol/L celecoxib, 200 μmol/L diclofenac, 50 μmol/L finasteride, 200 μmol/L flufenamic acid, 40 μmol/L meloxicam, 50 μmol/L ebselen, and 20 nmol/L flurbiprofen or DMSO. *Columns,* mean of triplicate independent experiments for each treatment; *bars,* SD. *OD,* absorbance.

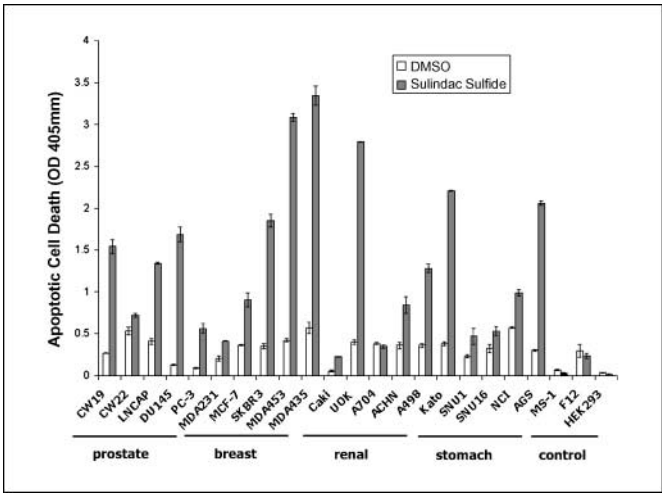

Figure 2. The NSAID sulindac sulfide induces apoptosis in cancer cells. Apoptosis assay of prostate, breast, renal, and stomach cancer cells. Cells were treated with 50 μmol/L sulindac sulfide or DMSO. Apoptosis was measured 24 hours posttreatment. *Columns,* mean of triplicate independent experiments for each treatment; *bars,* SD.

therefore, decided to evaluate whether the sulindac sulfide steady plasma concentration achievable in patients (43) was still able to induce apoptosis in cancer cells. Prostate cancer cells were treated with 5, 10, 25, and 50 μmol/L sulindac sulfide, and apoptosis was measured 24 hours posttreatment. We show that even low concentrations (5–10 μmol/L) of sulindac sulfide are sufficient to induce apoptosis in cancer cells (Supplementary Fig. S4*A*).

The proapoptotic cytokine MDA-7/IL-24 is the critical mediator of NSAID-induced apoptosis and growth arrest in cancer cells and inhibition of tumor growth *in vivo*. To elucidate the detailed molecular mechanisms underlying NSAID-mediated cell cycle arrest and apoptosis in cancer cells, we did oligonucleotide microarray-based transcriptional profiling of DU145 and PC-3 cells treated with 50 μmol/L sulindac sulfide versus DMSO. Detailed bioinformatic analysis revealed that sulindac sulfide does not trigger indiscriminate transcriptional shutdown of cancer cells, but induces distinct patterns of gene expression changes for a wide range of transcripts related to apoptosis and cell cycle (Supplementary Table S1[5]) that were consistent across the two cell lines, further confirming their apparent relevance for the cell cycle and cell death effects of sulindac sulfide.

Particularly striking and unanticipated was the dramatic up-regulation of the proapoptotic cytokine IL-24, also named MDA-7 (18, 19). *MDA-7/IL-24* was by far the highest up-regulated gene in both cell lines (140-fold in PC-3 and 722-fold in DU145). *MDA-7/IL-24* has been shown to be a novel tumor-suppressor gene (19, 44). At low, presumably physiologic concentrations, MDA-7/IL-24 functions predominantly as a cytokine involved in immunoregulation (19, 44). However, when overexpressed at supraphysiologic levels using an adenovirus vector, MDA-7/IL-24 shows cancer cell–specific growth inhibitory properties without negatively affecting normal cells (19, 21, 44, 45). Furthermore, elevated endogenous MDA-7/IL-24 expression correlates with enhanced apoptosis and prolonged overall survival of patients with small-cell lung cancer, further supporting the anticancer role of MDA-7/IL-24 (46). To evaluate the functional relevance of MDA-7/IL-24 induction for NSAID-mediated apoptosis, we measured mRNA expression levels of *MDA-7/IL-24* in response to sulindac sulfide in the same cancer cell lines tested above for apoptosis induction by sulindac sulfide. Real-time PCR analysis showed that sulindac sulfide induces *MDA-7/IL-24* expression in a variety of cancer types, up to 124-fold in DU145 cells and ~10- to 20-fold in various other cancer cell lines (Fig. 3*A*). Induction of *MDA-7/IL-24* by sulindac sulfide correlated with the ability of this drug to induce extensive apoptosis in these cell lines (Fig. 2*A*). Furthermore, sulindac sulfide induced *MDA-7/IL-24* gene expression as early as 8 hours posttreatment, before induction of programmed cell death at 12 hours posttreatment (Supplementary Fig. S3*A* and *B*).

These results indicate that sulindac sulfide–mediated induction of *MDA-7/IL-24* expression is a common pathway in various types of cancer cells that respond to this NSAID by undergoing apoptosis and strongly suggest that *MDA-7/IL-24* may play a critical role in this apoptosis induction.

To evaluate the relationship between MDA-7/IL-24 induction and apoptosis induction by various NSAIDs, we measured mRNA expression levels of *MDA-7/IL-24* in response to different NSAIDs in prostate cancer cells. Real-time PCR analysis showed that induction of *MDA-7/IL-24* is common to NSAIDs that induce apoptosis in cancer cells, because multiple, structurally unrelated NSAIDs strongly induced *MDA-7/IL-24* expression in DU145 prostate carcinoma cells (Fig. 3*B*) in strong correlation with NSAID-mediated apoptosis induction (correlation coefficient, 0.91; $P < 0.0001$). NSAIDs that strongly enhanced apoptosis (Fig. 1) dramatically induced *MDA-7/IL-24* expression (Fig. 3*B*), whereas NSAIDs that only marginally induced apoptosis (Fig. 1) did not significantly enhance *MDA-7/IL-24* expression (Fig. 3*B*). These data suggest a common mechanism for structurally unrelated NSAIDs in targeting MDA-7/IL-24 induction and apoptosis induction.

We and others have shown (19, 21, 44, 45) that overexpression of MDA-7/IL-24 following infection with an adenovirus carrying the *MDA-7/IL-24* gene induces apoptosis and inhibits cell proliferation in cancer cells (Supplementary Fig. S5*A* and *B*). To determine whether induction of growth arrest and apoptosis in cancer cells by NSAIDs is dependent on MDA-7/IL-24 up-regulation, we generated siRNA oligonucleotides and a lentivirus encoding this siRNA against MDA-7/IL-24. The specificity of the MDA-7/IL-24 siRNA oligonucleotides was validated as described in Supplementary Methods and Supplementary Fig. S5*C*. Infection with the LV-siRNA MDA-7/IL-24 reduced apoptosis induction by multiple NSAIDs by 90% (Fig. 3*C*) and reversed to a large part the G_2-M cell cycle arrest (Fig. 3*D*). These results show that MDA-7/IL-24 may play an important role in tumor cell survival and, for the first time, implicate MDA-7/IL-24 as an essential mediator of NSAID action in cancer cells.

To determine whether NSAIDs reduce tumor growth *in vivo* and to evaluate whether their effects may be dependent on induction of MDA-7/IL-24, prostate cancer cells stably infected with LV-siRNA GFP or LV-siRNA MDA-7/IL-24, as well as uninfected cells, were orthotopically implanted into the prostate of SCID mice. The mice were randomly divided into two groups and fed one of two diets through the entire experiment: AIN-93G as the control and the AIN-93G diet supplemented with 200 ppm sulindac sulfide. Two months later, the animals were examined for tumor formation and tumor weight. All mice developed tumors, indicating that this particular dose of sulindac sulfide did not prevent tumor formation. As seen in Fig. 3*E*, infection of DU145 cells with the

[5] www.bidmcgenomics.org/SulindacSulfide.

LV-siRNA GFP virus did not affect tumor growth in the control diet group, because implantation of uninfected DU145 cells showed a similar pattern of tumor growth and tumor weight when compared with the LV-siRNA GFP group (Fig. 3*E*). Surprisingly, the blockage of MDA-7/IL-24 expression by siRNA interference in the LV-siRNA MDA-7/IL-24 group strongly enhanced tumor growth, demonstrating that the low endogenous basal MDA-7/IL-24 expression acts as a tumor suppressor (P = 0.010; Fig. 3*E*). Tumor weight markedly increased by 60% in the LV-siRNA MDA-7/IL-24 group fed with the control diet when compared with the LV-siRNA GFP group (0.969 versus 0.623 g; P = 0.010).

Sulindac sulfide treatment reduced the average tumor weight in the LV-siRNA GFP group by 38% when compared with the control diet, confirming its antitumor efficacy (Fig. 3*E*). Sulindac sulfide treatment also reduced tumor growth in the LV-siRNA MDA-7/IL-24 group to some extent; however, tumor weight was still 75% higher than in the sulindac-treated LV-siRNA GFP group (P = 0.024; Fig. 3*E*). These results indicate that NSAID-mediated MDA-7/IL-24

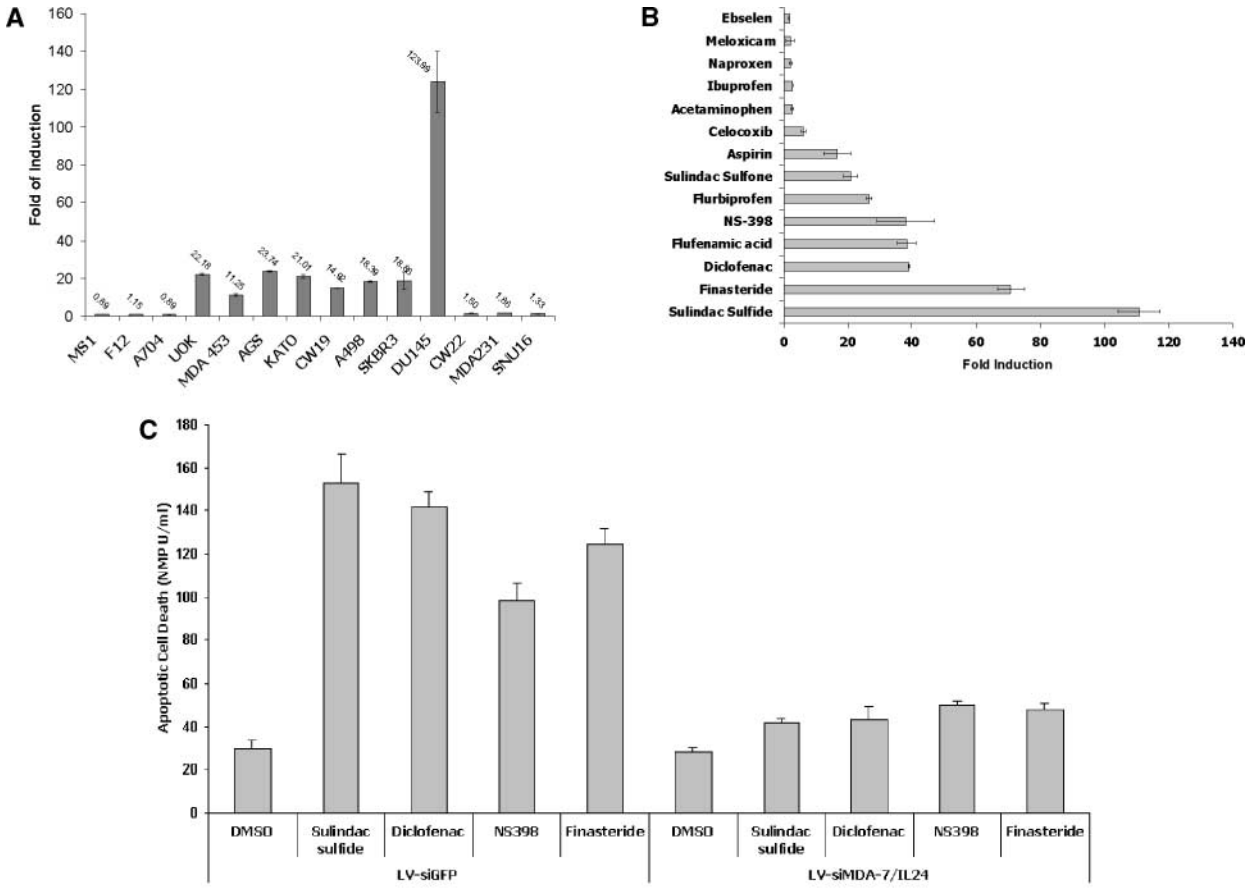

D

G1	G2	S	
57.28	**14.63**	28.08	siGFP/DMSO
42.70	**37.84**	19.46	siGFP/Sulindac sulifde
41.56	**38.87**	19.57	siGFP/Diclofenac
39.10	**39.70**	21.20	siGFP/NS-398
59.89	**15.56**	24.55	siIL24/Sulindac
62.73	**13.89**	23.38	siIL24/Diclofenac
60.95	**15.91**	23.13	siIL24/NS-398
61.57	**14.10**	24.33	siIL24/DMSO

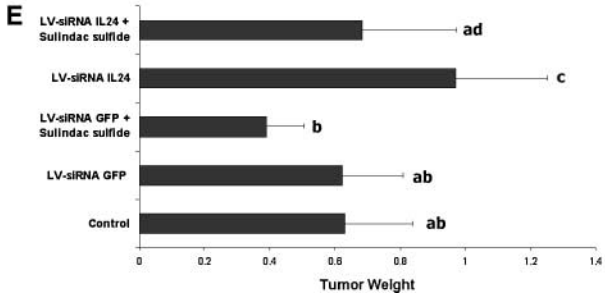

Figure 3. MDA-7/IL-24 is the crucial mediator of NSAID-induced growth arrest and apoptosis in cancer cells and inhibition of tumor growth *in vivo. A,* sulindac sulfide induces *MDA-7/IL-24* expression in various types of cancer cells. Real-time PCR of *MDA-7/IL-24* after 24 hours of sulindac sulfide treatment. Each sample was normalized to *hGAPDH. B,* real-time PCR analysis of MDA-7/IL-24 expression in DU145 cells after 24 hours of treatment with different NSAIDs. Each sample was normalized to hGAPDH. *C,* apoptosis assay of PC-3 cells after treatment with 50 μmol/L sulindac sulfide, 40 μmol/L diclofenac, 200 μmol/L NS398, and 50 μmol/L finasteride or DMSO, and infection with lentivirus encoding MDA-7/IL-24 siRNA duplexes. *Columns,* mean of triplicate independent infection for each vector at each treatment; *bars,* SD. *D,* cell cycle analysis in DU145 and PC-3 cells treated with 50 μmol/L sulindac sulfide or DMSO and transfected with MDA-7/IL-24 siRNA duplexes. The percentages of cells in a particular cell cycle phase were determined by fluorescence-activated cell sorting analysis 24 hours after treatment. *E, MDA-7/IL-24* is a tumor suppressor and contributes to sulindac sulfide–mediated inhibition of tumor growth. For each inoculation, 2×10^6 DU145 cells infected with LV-siRNA GFP, LV-siRNA IL-24, or uninfected cells were orthotopically implanted into the prostate of SCID mice. The mice were randomly divided into two groups (n = 8 per group) and fed one of two diets through the entire experiment: AIN-93G as the control and the AIN-93G diet supplemented with 200 ppm sulindac sulfide. The size of the tumors and tumor weight were measured 2 months after implantation. Values not sharing the same letters are statistically significant with P values at least <0.05.

induction plays a critical role in tumor growth and also indicate a tumor-suppressor activity of MDA-7/IL-24.

Induction of the *GADD45α* and *GADD45γ* genes is tightly regulated by *MDA-7/IL-24* in NSAID-treated cancer cells. Our transcriptional profiling experiments, moreover, showed a strong up-regulation of GADD45α up to 16-fold by sulindac sulfide (Supplementary Table S1). MDA-7/IL-24 regulates and induces GADD45α and GADD45γ without affecting GADD45β expression (refs. 20, 21; Supplementary Fig. S6), and we have previously shown that GADD45α and GADD45γ up-regulation upon inhibition of nuclear factor-κB (NF-κB) is critical for induction of apoptosis in cancer cells (20). The *GADD45* gene family encodes three structurally highly related growth arrest– and DNA damage–inducible proteins, GADD45α, GADD45β, and GADD45γ (47), which play a role in the G_2-M checkpoint in response to DNA damage (48).

To evaluate whether regulation of *GADD45* genes is involved in NSAID-mediated apoptosis and whether *GADD45α* and *GADD45γ* regulation is a result of MDA-7/IL-24 induction by NSAIDs, expression of *GADD45* family members was measured by real-time PCR in the different cancer cell lines treated with sulindac sulfide (Fig. 4*A*). Whereas *GADD45β* expression was not significantly affected by sulindac sulfide in any of the cell lines, the drug induced *GADD45α* and *GADD45γ* expression 1.5- to 27-fold in various cancer cell types, indicating that *GADD45α* and *GADD45γ* expression is consistently regulated by sulindac sulfide (Fig. 4*A*). Furthermore, up-regulation of *GADD45α* and GADD45γ strongly correlated with the ability of sulindac sulfide to induce *MDA-7/IL-24* expression (correlation coefficient, 0.63; $P = 0.016$; correlation coefficient, 0.69; $P = 0.0068$, respectively; Fig. 3*A*). Interestingly, the correlation between induction of *GADD45α* and *GADD45γ* was also significant (correlation coefficient, 0.85; $P = 0.0001$).

Differences in mRNA expression of the GADD45 family members were corroborated on the protein level by Western blot analysis using protein extracts from DU145 and PC-3 cells treated with sulindac sulfide for 24 hours. GADD45α and GADD45γ, but not GADD45β? protein expression, were induced in sulindac sulfide–treated cancer cells (Fig. 4*B*).

To evaluate whether NSAID-mediated induction of GADD45α and GADD45γ expression is dependent on MDA-7/IL-24 up-regulation, we transfected prostate cancer cells with MDA-7/IL-24 siRNA oligonucleotides and measured *GADD45* expression 24 hours after treatment with sulindac sulfide by real-time PCR. Interference with MDA-7/IL-24 expression almost completely blocked sulindac sulfide–mediated induction of *GADD45α* and *GADD45γ* gene expression without affecting *GADD45β* expression (Fig. 4*C*). These data most vividly show that GADD45α and GADD45γ induction by sulindac sulfide is mediated via MDA-7/IL-24 up-regulation.

Inhibition of NF-κB also has been shown to induce apoptosis due to up-regulation of GADD45α and GADD45γ (20). Surprisingly, treatment of prostate cancer cells with sulindac sulfide had no effect on the NF-κB signaling pathways (Supplementary Fig. S7*A* and S7*B*).

NSAID-mediated GADD45α and GADD45γ induction is essential for Cdc2 kinase activation and growth arrest. Our transcriptional profiling analysis showed that, in concordance with the observed G_2-M cell cycle arrest induced by sulindac sulfide, several genes involved in the G_2-M checkpoint and Cdc2 kinase regulation are down-regulated by sulindac sulfide, including Cdc25C, Cdc2, cyclin B1, and cyclin B2, whereas the cyclin-dependent kinase inhibitor p21 is up-regulated (Supplementary Table S1). Western blot analysis of protein extracts from DU145 and PC-3 cells treated with

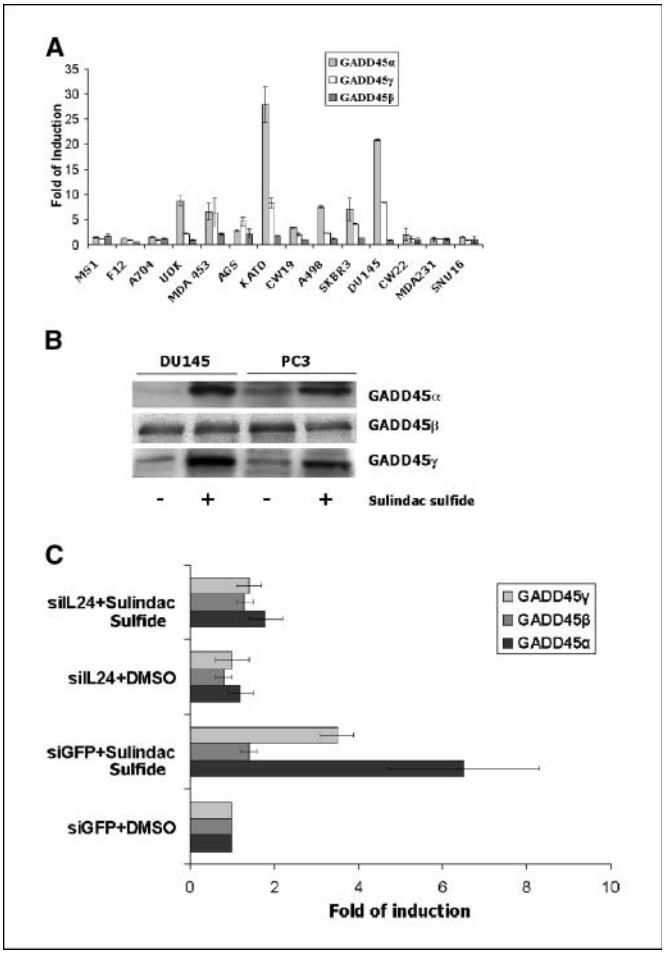

Figure 4. Expression of the GADD45 family members is tightly regulated by NSAIDs through induction of MDA-7/IL-24. *A,* real-time PCR analysis of *GADD45α, GADD45β,* and *GADD45γ* expression after treatment with 50 μmol/L sulindac sulfide or DMSO in prostate, breast, renal, and stomach cancer cell lines. Each sample was normalized to *hGAPDH. B,* Western blot analysis of GADD45 family members in response to sulindac sulfide treatment. Protein extracts were obtained 24 hours after treatment of prostate cancer cells with 50 μmol/L sulindac sulfide or DMSO. *C,* real-time PCR analysis of *GADD45α, GADD45β,* and *GADD45γ* expression after treatment of DU145 and PC-3 cells with 50 μmol/L sulindac sulfide or DMSO and transfection of MDA-7/IL-24 siRNA duplex (50 nmol/L) in prostate cancer cell lines. Each sample was normalized to *hGAPDH*.

sulindac sulfide for 24 hours corroborated the expression changes on the protein level. Protein expression of Cdc25C, cyclin B1, and cyclin B2 decreased, and p21 protein expression increased, in response to sulindac sulfide (Fig. 5*A*). GADD45α has been shown to inhibit the kinase activity of the Cdc2-cyclin B complex (49) and progression from the G2 to the M phase of the cell cycle (50). To determine the role of GADD45α and GADD45γ in NSAID-induced G_2-M arrest, we infected DU145 prostate cancer cells with lentiviruses encoding siRNAs for *GADD45α, GADD45γ,* or *GFP*. An *in vitro* Cdc2 kinase assay was done with whole-cell lysates from these infected cells after treatment with sulindac sulfide or DMSO for 24 hours using histone H1 as the Cdc2 substrate. Active Cdc2 directly correlates with enhanced phosphorylation of histone H1. A significant level of phosphorylated histone H1 in untreated cells infected with the control lentivirus indicated significant Cdc2 activity in proliferating DU145 cells (Fig. 5*B*). Cdc2 activity was substantially decreased 24 hours after sulindac sulfide treatment correlating with enhanced

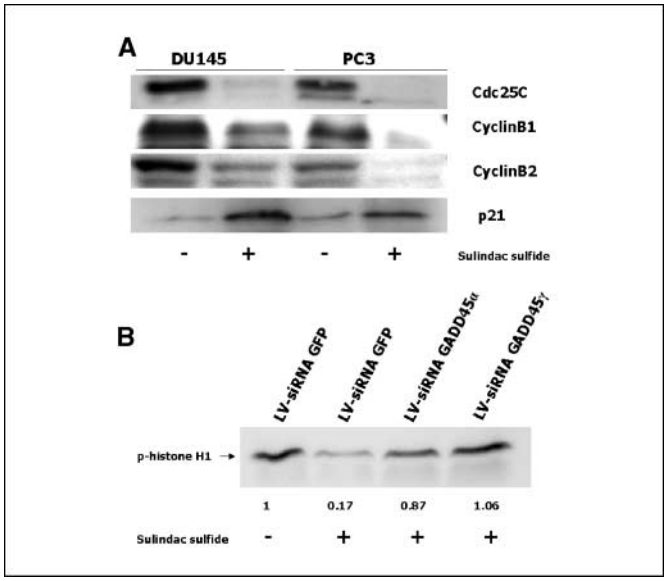

Figure 5. Sulindac sulfide–induced GADD45 expression is essential for growth arrest induction by altering the Cdc2-cyclin B checkpoint. *A,* regulation of genes involved in the Cdc2-cyclin B signaling pathway by sulindac sulfide. Western blot analysis of Cdc25C, cyclin B1, cyclin B2, and p21 proteins in DU145 and PC-3 cells treated for 24 hours with 50 μmol/L sulindac sulfide or DMSO. *B,* inhibition of Cdc2 activation in response to sulindac sulfide treatment is due to induction of GADD45α and GADD45γ. Phosphorylation of the Cdc2 substrate histone H1 by the Cdc2-cyclin B complex in PC-3 cells 24 hours after treatment with 50 μmol/L sulindac sulfide and infections with GADD45α and GADD45γ LV-siRNAs.

GADD45α and GADD45γ expression and G_2-M arrest. However, inhibition of GADD45α and GADD45γ expression in DU145 cells by the LV-siRNAs restored Cdc2 kinase activity as seen by increased histone H1 phosphorylation (Fig. 5*B*). These data suggest that sulindac sulfide–induced G_2-M cell cycle arrest is due to a combination of decreased expression of several G_2-M transition cell cycle regulators and MDA-7/IL-24–induced GADD45α and GADD45γ up-regulation that leads to inhibition of Cdc2 activity.

MDA-7/IL-24–dependent GADD45α and GADD45γ induction and JNK activation are critical for NSAID-mediated apoptosis induction in cancer cells. To elucidate the functional relevance of GADD45α and GADD45γ for NSAID-mediated apoptosis, we measured apoptosis induction by sulindac sulfide in GADD45α and GADD45γ knockdown cells. siRNA-mediated inhibition of sulindac sulfide induced up-regulation of GADD45α or GADD45γ expression and almost completely abrogated apoptosis induction (Fig. 6*A*), clearly demonstrating the absolute requirement of MDA-7/IL-24–dependent GADD45α and GADD45γ up-regulation for apoptosis induction by NSAIDs.

Because we and others had shown that JNK activation plays a role in apoptosis induction in cancer cells and GADD45α and GADDγ interact with the upstream kinase of JNK, mitogen-activated protein kinase kinase kinase 4, and activate JNK (47), we evaluated the relevance of JNK for NSAID-mediated apoptosis. JNK kinase activity was tested in protein extracts obtained from DU145 and PC-3 cells treated with sulindac sulfide or DMSO for 24 hours by an *in vitro* kinase assay. Western blot analysis revealed very little JNK activity in untreated control cells and a strong increase in JNK activity in both cell lines upon treatment with sulindac sulfide (Fig. 6*B*). JNK activation by sulindac sulfide was at least partially dependent on MDA-7/IL-24 induction because JNK activity in sulindac sulfide–treated *MDA-7/IL-24−/−* cells was reduced by 62%, but not completely abolished when compared with *MDA-7/IL-24+/+* cells (Fig. 6*C*). The importance of GADD45α and GADD45γ for NSAID-induced JNK activation was evaluated in DU145 and PC-3 cells infected with the GADD45α or GADD45γ siRNA lentiviruses or the control lentivirus and treated with sulindac sulfide for 24 hours. Inhibition of sulindac sulfide–mediated up-regulation of GADD45α and GADD45γ expression by siRNA drastically reduced JNK activation in both cell lines, correlating with the inhibition of apoptosis induction (Fig. 6*D*).

To establish the relevance of JNK activation in mediating apoptosis in cancer cells, apoptosis was measured in protein extracts obtained from DU145 and PC-3 cells treated with 50 μmol/L sulindac sulfide or DMSO in the absence or presence of a specific JNK inhibitor, JNKII. Compared with controls, apoptosis of sulindac sulfide–treated cells was reduced by >56% in DU145 cells and 40% in PC-3 cells in JNKII-treated cells, but inhibition of JNK did not fully abolish apoptosis induction (Fig. 6*E*). These results suggest that JNK contributes to, but is not absolutely essential for, sulindac sulfide–mediated apoptosis.

Discussion

Dissection of the biological and biochemical pathways targeted by NSAIDs will provide ample opportunities to screen for chemically modified NSAIDs or for new compounds that are more effective and specific in destroying cancer cells. Furthermore, NSAID treatments have been reported to induce changes in gene expression in a variety of cancer cells affecting multiple target genes (51–54). We report here the discovery of a novel biological pathway involving MDA-7/IL-24 and the GADD45 gene family that are targeted by a set of NSAIDs in a number of cancer types and whose activation directly correlates with the efficacy of NSAIDs to induce cancer cell death. We show that multiple classes of structurally unrelated NSAIDs induce apoptosis and growth arrest via induction of MDA-7/IL-24 expression with consecutive GADD45α and GADD45γ induction, leading to JNK activation and GADD45α- and GADD45γ-dependent inhibition of Cdc2 activity (Fig. 6*F*).

Several studies using an adenovirus encoding the *MDA-7/IL-24* gene show its profound and selective anticancer activity *in vitro* and in animal models (19, 21, 44, 45, 55). However, transient expression, frequent adverse immune reactions, and limitations to local delivery may restrict the use of adenoviral delivery of *MDA-7/IL-24*. This potential problem is partly ameliorated by the potent "bystander antitumor" activity of MDA-7/IL-24 mediated by its cytokine properties (19, 44, 56, 57). In these contexts, our discovery of specific high-level induction of MDA-7/IL-24 in different types of cancer cells, by a variety of NSAIDs, provides a new entry point to enhance MDA-7/IL-24 levels in cancer cells on a systemic level that should be significantly more effective than adenoviral delivery. Additionally, recent studies correlate increased levels of endogenous MDA-7/IL-24 with a favorable prognosis in lung adenocarcinoma and a significantly higher incidence of apoptotic tumor cells (46) and treatment of human lung tumor xenografts in nude mice with Ad-MDA-7/IL-24 plus sulindac suppressed growth more efficiently than Ad-MDA-7/IL-24 or sulindac alone (58). Therefore, our findings that NSAIDs induce high levels of MDA-7/IL-24 in various types of cancers and use the potent proapoptotic activity of MDA-7/IL-24 to induce apoptosis and cell cycle arrest in cancer cells strongly support the notion that therapeutic strategies that lead to enhanced MDA-7/IL-24 expression in cancer cells will have a significant effect on cancer patient survival.

Our *in vivo* orthotopic tumor model provides further support of the hypothesis that *MDA-7/IL-24* is indeed a tumor-suppressor gene. Blocking MDA-7/IL-24 expression by siRNA interference not only reduced the ability of sulindac sulfide to inhibit tumor growth *in vivo*, but also enhanced tumor growth in the LV-siRNA MDA-7/IL-24 group. However, sulindac sulfide, to some extent, still inhibited tumor growth in animals receiving LV-siRNA MDA-7/IL-24. This partial *in vivo* effect of sulindac sulfide on tumor growth following injection with tumor cells expressing the MDA-7/IL-24 siRNA could be explained by several mechanisms: Although MDA-7/IL-24 expression was inhibited in the tumor cells, systemic sulindac sulfide exposure in the mice led to MDA-7/IL-24 expression in mouse-derived cells or tissues that affected the implanted tumor cells and partially reversed the effect of the

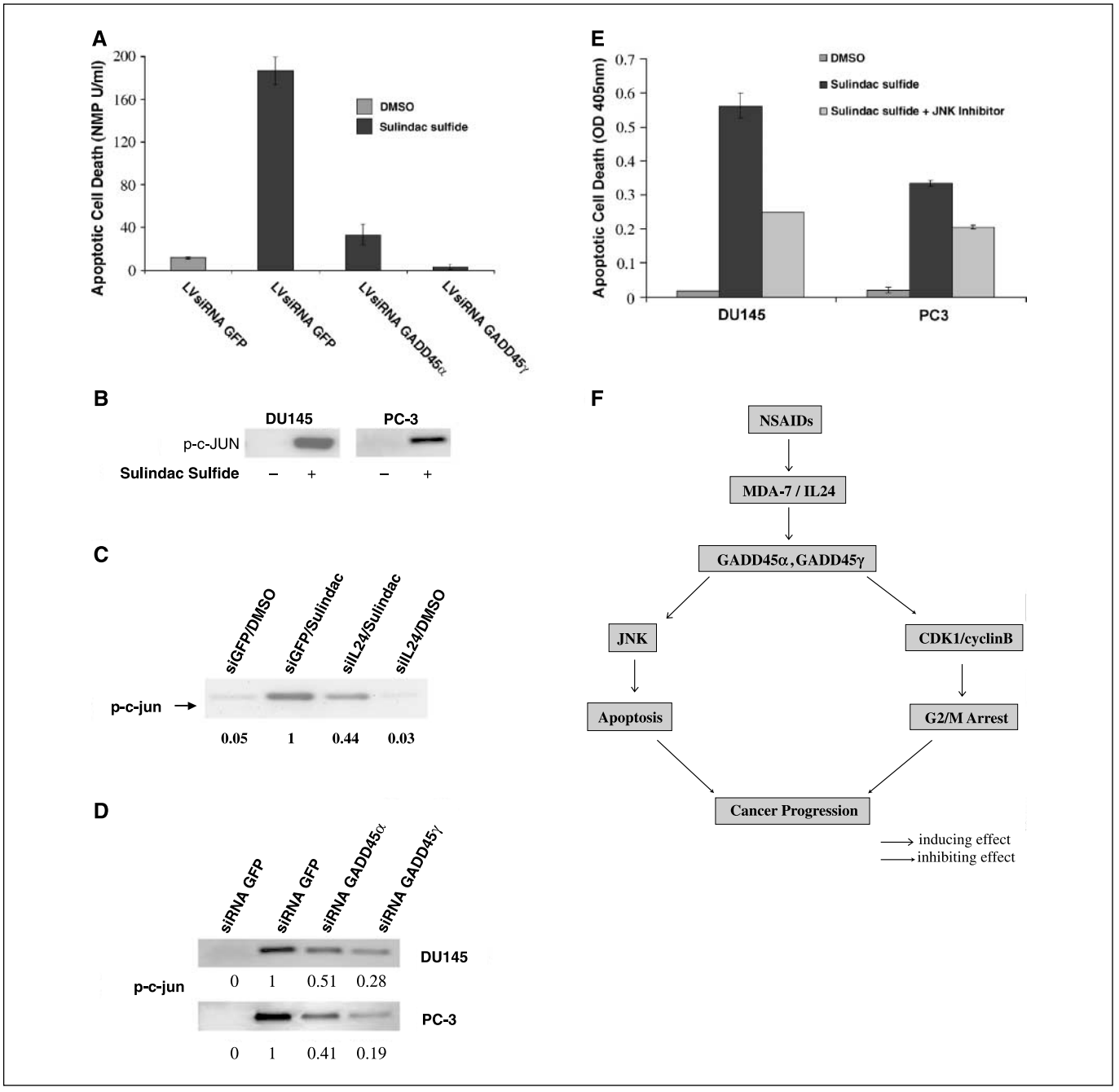

Figure 6. Induction of GADD45 expression by NSAIDs is essential for JNK activation and apoptosis induction. *A,* apoptosis assay of PC-3 cells after treatment with 50 μmol/L sulindac sulfide or DMSO and infection with GADD45α and GADD45γ LV-siRNAs. *Columns,* mean of triplicate independent infections for each vector at each treatment; *bars,* SD. *B,* induction of JNK activation by sulindac sulfide. JNK kinase was analyzed in cell lysates from DU145 and PC-3 cells treated with 50 μmol/L sulindac sulfide or DMSO using the SAPK/JNK assay kit (Cell Signaling). *C,* kinase assay showing inhibition of JNK kinase activity by MDA-7/IL-24 siRNA (50 μmol/L) in prostate cancer cells treated with 50 μmol/L sulindac sulfide or DMSO. *D,* kinase assay showing inhibition of JNK kinase activity by GADD45 siRNA duplexes (50 μmol/L) in prostate cancer cells treated with 50 μmol/L sulindac sulfide or DMSO. *E,* apoptosis of prostate cancer cells 24 hours after treatment with 50 μmol/L sulindac sulfide or DMSO and treatment with the JNK inhibitor JNKII SP600125 (100 nmol/L; Calbiochem). *Columns,* mean of triplicate independent treatments; *bars,* SD. *F,* schematic presentation of NSAID signaling pathway in cancer.

MDA-7/IL-24 siRNA; it is also likely that MDA-24/IL-24 is not the sole pathway targeted by sulindac sulfide and the drug could act through multiple pathways to induce programmed cell death in cancer cells, including indirect antitumor effects on stromal and vascular cells.

Additionally, our data provide strong evidence that multiple NSAIDs induce cancer cell death through MDA-7/IL-24–mediated up-regulation of GADD45α and GADD45γ, irrespective of their ability to block COX-2. For example, finasteride, a selective 5-α-reductase inhibitor (59), is not known to inhibit COX-2 but strongly induces MDA-7/IL-24 expression and apoptosis, whereas the potent selective COX-2 inhibitor celecoxib is significantly less effective in inducing MDA-7/IL-24 and apoptosis. On the other hand, the nonselective cation channel blocker flufenamic acid and the nonselective COX-1 and COX-2 inhibitors sulindac sulfide and diclofenac are very potent inducers of MDA-7/IL-24 and apoptosis. Thus, the proapoptotic anticancer activity of several divergent classes of drugs evaluated here seems not to be due primarily to their effects on their supposed targets, but due to the off-target induction of MDA-7/IL-24.

Inhibition of NF-κB in the same cell lines tested here induced apoptosis without inducing MDA-7/IL-24, although up-regulation of GADD45α and GADD45γ via repression of c-myc expression was as essential for apoptosis induction as in response to NSAIDs (20) and multiple MDA-7/IL-24–dependent and MDA-7/IL-24–independent pathways seem to merge into GADD45α and GADD45γ. Although current studies indicate that members of the GADD45 family appear infrequently mutated in cancer, reduced GADD45 expression due to gene and or promoter methylation have been frequently observed in several types of human cancer (60, 61).

In conclusion, the ability of NSAIDs to induce apoptosis seems to depend on their abilities to induce MDA-7/IL-24 expression and enhance GADD45α and GADD45γ expression. Thus, apoptosis and growth arrest induction of cancer cells as a result of enhanced MDA-7/IL-24 expression seems to be a common pathway for multiple classes of drugs. These results also provide a rationale to screen small-molecule libraries, natural compound libraries, and chemically modified NSAIDs for selective inducers of MDA-7/IL-24 expression in cancer cells to obtain more effective anticancer drugs.

Acknowledgments

Received 6/13/2006; revised 9/6/2006; accepted 10/9/2006.

Grant support: NIH grants 1RO1 CA85467, P50 CA090381, P50 CA105009, and the Hershey Foundation (T.A. Libermann); NIH grants 1R01 CA097318, 1R01 CA098712, P01 CA104177, the Samuel Waxman Cancer Research Foundation, and the Chernow Endowment (P.B. Fisher); and Department of Defense grant PC051217 (L.F. Zerbini).

The costs of publication of this article were defrayed in part by the payment of page charges. This article must therefore be hereby marked *advertisement* in accordance with 18 U.S.C. Section 1734 solely to indicate this fact.

We thank Dr. Inder M. Verma for help with the generation of lentiviruses.

References

1. Umar A, Viner JL, Anderson WF, Hawk ET. Development of COX inhibitors in cancer prevention and therapy. Am J Clin Oncol 2003;26:S48–57.
2. Harris RE, Beebe-Donk J, Doss H, Doss DB. Aspirin, ibuprofen, and other non-steroidal anti-inflammatory drugs in cancer prevention: a critical review of non-selective COX-2 blockade [review]. Oncol Rep 2005;13: 559–83.
3. Taketo MM. Cyclooxygenase-2 inhibitors in tumorigenesis. J Natl Cancer Inst 1998;90:1529–36.
4. Baron JA, Cole BF, Sandler RS, et al. A randomized trial of aspirin to prevent colorectal adenomas. N Engl J Med 2003;348:891–9.
5. Saji S, Hirose M, Toi M. Novel sensitizing agents: potential contribution of COX-2 inhibitor for endocrine therapy of breast cancer. Breast Cancer 2004;11:129–33.
6. Wechter WJ, Kantoci D, Murray ED, Jr., et al. R-Flurbiprofen chemoprevention and treatment of intestinal adenomas in the APC(Min)/+ mouse model: implications for prophylaxis and treatment of colon cancer. Cancer Res 1997;57:4316–24.
7. Narayanan BA, Narayanan NK, Pittman B, Reddy BS. Regression of mouse prostatic intraepithelial neoplasia by nonsteroidal anti-inflammatory drugs in the transgenic adenocarcinoma mouse prostate model. Clin Cancer Res 2004;10:7727–37.
8. Lin DW, Nelson PS. The role of cyclooxygenase-2 inhibition for the prevention and treatment of prostate carcinoma. Clin Prostate Cancer 2003;2:119–26.
9. Mann JR, DuBois RN. Cyclooxygenase-2 and gastrointestinal cancer. Cancer J 2004;10:145–52.
10. Basler JW, Piazza GA. Nonsteroidal anti-inflammatory drugs and cyclooxygenase-2 selective inhibitors for prostate cancer chemoprevention. J Urol 2004;171: S59–62; discussion S62–53.
11. Sabichi AL, Lippman SM. COX-2 inhibitors and other nonsteroidal anti-inflammatory drugs in genitourinary cancer. Semin Oncol 2004;31:36–44.
12. Song X, Lin HP, Johnson AJ, et al. Cyclooxygenase-2, player or spectator in cyclooxygenase-2 inhibitor-induced apoptosis in prostate cancer cells. J Natl Cancer Inst 2002;94:585–91.
13. Haanen C. Sulindac and its derivatives: a novel class of anticancer agents. Curr Opin Investig Drugs 2001;2: 677–83.
14. Kashfi K, Ryann Y, Qiao LL, et al. Nitric oxide-donating nonsteroidal anti-inflammatory drugs inhibit the growth of various cultured human cancer cells: evidence of a tissue type-independent effect. J Pharmacol Exp Ther 2002;303:1273–82.
15. Xiao D, Deguchi A, Gundersen GG, Oehlen B, Arnold L, Weinstein IB. The sulindac derivatives OSI-461, OSIP486823, and OSIP487703 arrest colon cancer cells in mitosis by causing microtubule depolymerization. Mol Cancer Ther 2006;5:60–7.
16. Marx J. Cancer research. Anti-inflammatories inhibit cancer growth—but how? Science 2001;291:581–2.
17. Elder DJ, Halton DE, Hague A, Paraskeva C. Induction of apoptotic cell death in human colorectal carcinoma cell lines by a cyclooxygenase-2 (COX-2)-selective nonsteroidal anti-inflammatory drug: independence from COX-2 protein expression. Carcinogenesis 2001;22:17–25.
18. Jiang H, Lin JJ, Su Z-Z, Goldstein NI, Fisher PB. Subtraction hybridization identifies a novel melanoma differentiation associated gene, mda-7, modulated during human melanoma differentiation, growth and progression. Oncogene 1995;11:2477–86.
19. Fisher PB. Is *mda*-7/IL-24 a "magic bullet" for cancer? Cancer Res 2005;65:10128–38.
20. Zerbini LF, Wang Y, Czibere A, et al. NF-κ B-mediated repression of growth arrest- and DNA-damage-inducible proteins 45α and γ is essential for cancer cell survival. Proc Natl Acad Sci U S A 2004;101:13618–23.
21. Sarkar D, Su ZZ, Lebedeva IV, et al. mda-7 (IL-24) Mediates selective apoptosis in human melanoma cells by inducing the coordinated overexpression of the GADD family of genes by means of p38 MAPK. Proc Natl Acad Sci U S A 2002;99:10054–9.
22. Ramalho-Santos M, Yoon S, Matsuzaki Y, Mulligan RC, Melton DA. "Stemness": transcriptional profiling of embryonic and adult stem cells. Science 2002;298:597–600.
23. Li C, Wong WH. Model-based analysis of oligonucleotide arrays: expression index computation and outlier detection. Proc Natl Acad Sci U S A 2001;98:31–6.
24. Yuen T, Wurmbach E, Pfeffer RL, Ebersole BJ, Sealfon SC. Accuracy and calibration of commercial oligonucleotide and custom cDNA microarrays. Nucleic Acids Res 2002;30:e48.
25. Ravis WR, Diskin CJ, Campagna KD, Clark CR, McMillian CL. Pharmacokinetics and dialyzability of sulindac and metabolites in patients with end-stage renal failure. J Clin Pharmacol 1993;33:527–34.
26. Roberts DG, Gerber JG, Barnes JS, Zerbe GO, Nies AS. Sulindac is not renal sparing in man. Clin Pharmacol Ther 1985;38:258–65.
27. Swanson BN, Boppana VK, Vlasses PH, Holmes GI, Monsell K, Ferguson RK. Sulindac disposition when given once and twice daily. Clin Pharmacol Ther 1982; 32:397–403.
28. Ray GF, Lanman RC, Fu CJ, Paranka NS, Pamukcu R, Wheeler SC. Determination of FGN-1 (an active metabolite of Sulindac) in human plasma, urine, and feces by HPLC. J Pharm Biomed Anal 1995;14:213–20.
29. Khosravan R, Wu JT, Joseph-Ridge N, Vernillet L. Pharmacokinetic interactions of concomitant administration of febuxostat and NSAIDs. J Clin Pharmacol 2006;46:855–66.
30. Davies NM, Skjodt NM. Clinical pharmacokinetics of meloxicam. A cyclo-oxygenase-2 preferential nonsteroidal anti-inflammatory drug. Clin Pharmacokinet 1999; 36:115–26.
31. Yin MJ, Yamamoto Y, Gaynor RB. The anti-inflammatory agents aspirin and salicylate inhibit the activity of I(κ)B kinase-β. Nature 1998;396:77–80.
32. Lockwood GF, Albert KS, Gillespie WR, et al. Pharmacokinetics of ibuprofen in man. I. Free and total area/dose relationships. Clin Pharmacol Ther 1983;34:97–103.
33. Lentjes EG, van Ginneken CA. Pharmacokinetics of flufenamic acid in man. Int J Clin Pharmacol Ther 1987; 25:185–7.
34. Taburet AM, Singlas E, Glass RC, Thomas F, Leutenegger E. Pharmacokinetic comparison of oral and local action transcutaneous flurbiprofen in healthy volunteers. J Clin Pharm Ther 1995;20:101–7.
35. Terlinden R, Feige M, Romer A. Determination of the two major metabolites of ebselen in human plasma by high-performance liquid chromatography. J Chromatogr 1988;430:438–42.
36. Davies NM, McLachlan AJ, Day RO, Williams KM. Clinical pharmacokinetics and pharmacodynamics of celecoxib: a selective cyclo-oxygenase-2 inhibitor. Clin Pharmacokinet 2000;38:225–42.
37. Carlin JR, Hoglund P, Eriksson LO, et al. Disposition and pharmacokinetics of [14C]finasteride after oral administration in humans. Drug Metab Dispos 1992;20: 148–55.
38. Su SF, Chou CH, Kung CF, Huang JD. *In vitro* and *in vivo* comparison of two diclofenac sodium sustained release oral formulations. Int J Pharm 2003;260:39–46.

39. Kennedy JM, van Rij AM. Drug absorption from the small intestine in immediate postoperative patients. Br J Anaesth 2006;97:171–80.

40. Liu XH, Yao S, Kirschenbaum A, Levine AC. NS398, a selective cyclooxygenase-2 inhibitor, induces apoptosis and down-regulates bcl-2 expression in LNCaP cells. Cancer Res 1998;58:4245–9.

41. Williams CS, Goldman AP, Sheng H, Morrow JD, DuBois RN. Sulindac sulfide, but not sulindac sulfone, inhibits colorectal cancer growth. Neoplasia 1999;1:170–6.

42. Thun MJ, Henley SJ, Patrono C. Nonsteroidal anti-inflammatory drugs as anticancer agents: mechanistic, pharmacologic, and clinical issues. J Natl Cancer Inst 2002;94:252–66.

43. Davies NM, Watson MS. Clinical pharmacokinetics of sulindac. A dynamic old drug. Clin Pharmacokinet 1997; 32:437–59.

44. Gupta P, Su Z-Z, Lebedeva IV, et al. mda-7/IL-24: Multifunctional cancer-specific apoptosis-inducing cytokine. Pharmacol Ther 2006;111:596–628.

45. Su Z-Z, Lebedeva IV, Sarkar D, et al. Melanoma differentiation associated gene-7, mda-7/IL-24, selectively induces growth suppression, apoptosis and radiosensitization in malignant gliomas in a p53-independent manner. Oncogene 2003;22:1164–80.

46. Ishikawa S, Nakagawa T, Miyahara R, et al. Expression of MDA-7/IL-24 and its clinical significance in resected non-small cell lung cancer. Clin Cancer Res 2005;11:1198–202.

47. Mita H, Tsutsui J, Takekawa M, Witten EA, Saito H. Regulation of MTK1/MEKK4 kinase activity by its N-terminal autoinhibitory domain and GADD45 binding. Mol Cell Biol 2002;22:4544–55.

48. Jin S, Antinore MJ, Lung FD, et al. The GADD45 inhibition of Cdc2 kinase correlates with GADD45-mediated growth suppression. J Biol Chem 2000;275:16602–8.

49. Vairapandi M, Balliet AG, Hoffman B, Liebermann DA. GADD45b and GADD45g are cdc2/cyclinB1 kinase inhibitors with a role in S and G2/M cell cycle checkpoints induced by genotoxic stress. J Cell Physiol 2002;192:327–38.

50. Wang XW, Zhan Q, Coursen JD, et al. GADD45 induction of a G2/M cell cycle checkpoint. Proc Natl Acad Sci U S A 1999;96:3706–11.

51. Bottone FG, Jr., Martinez JM, Collins JB, Afshari CA, Eling TE. Gene modulation by the cyclooxygenase inhibitor, sulindac sulfide, in human colorectal carcinoma cells: possible link to apoptosis. J Biol Chem 2003; 278:25790–801.

52. Roy D, Panda A, Calaf GM, Mitra A. Differential gene expression of sulindac-treated human breast epithelial cells. Int J Oncol 2005;27:1727–36.

53. Gao XQ, Han JX, Huang HY, Song B, Zhu B, Song CZ. Effect of NS398 on metastasis-associated gene expression in a human colon cancer cell line. World J Gastroenterol 2005;11:4337–43.

54. Hardwick JC, van Santen M, van den Brink GR, van Deventer SJ, Peppelenbosch MP. DNA array analysis of the effects of aspirin on colon cancer cells: involvement of Rac1. Carcinogenesis 2004;25:1293–8.

55. Lebedeva IV, Su ZZ, Sarkar D, Fisher PB. Restoring apoptosis as a strategy for cancer gene therapy: focus on p53 and mda-7. Semin Cancer Biol 2003;13:169–78.

56. Su ZZ, Lebedeva IV, Gopalkrishnan RV, et al. A combinatorial approach for selectively inducing programmed cell death in human pancreatic cancer cells. Proc Natl Acad Sci U S A 2001;98:10332–7.

57. Su Z-Z, Emdad L, Sauane M, et al. Unique aspects of mda-7/IL-24 antitumor bystander activity: establishing a role for secretion of MDA-7/IL-24 protein by normal cells. Oncogene 2005;24:7552–66.

58. Oida Y, Gopalan B, Miyahara R, et al. Sulindac enhances adenoviral vector expressing mda-7/IL-24-mediated apoptosis in human lung cancer. Mol Cancer Ther 2005;4:291–304.

59. Wysowski DK, Farinas E. Finasteride in benign prostatic hyperplasia. N Engl J Med 2004;350:1359–61.

60. Bahar A, Bicknell JE, Simpson DJ, Clayton RN, Farrell WE. Loss of expression of the growth inhibitory gene GADD45γ, in human pituitary adenomas, is associated with CpG island methylation. Oncogene 2004;23: 936–44.

61. Sun L, Gong R, Wan B, et al. GADD45γ, down-regulated in 65% hepatocellular carcinoma (HCC) from 23 chinese patients, inhibits cell growth and induces cell cycle G2/M arrest for hepatoma Hep-G2 cell lines. Mol Biol Rep 2003;30:249–53.

Reduced PDEF Expression Increases Invasion and Expression of Mesenchymal Genes in Prostate Cancer Cells

Xuesong Gu,[1] Luiz F. Zerbini,[1] Hasan H. Otu,[1] Manoj Bhasin,[1] Quanli Yang,[2] Marie G. Joseph,[1] Franck Grall,[1] Tomi Onatunde,[1] Ricardo G. Correa,[3] and Towia A. Libermann[1]

[1]BIDMC Genomics Center, Beth Israel Deaconess Medical Center and Harvard Medical School, Boston, Massachusetts; [2]Medical Polymer Center, National Institute of Family Planning, Beijing, China; and [3]Laboratory of Genetics, The Salk Institute for Biological Studies, La Jolla, California

Abstract

The epithelium-specific Ets transcription factor, PDEF, plays a role in prostate and breast cancer, although its precise function has not been established. In prostate cancer, PDEF is involved in regulating prostate-specific antigen expression via interaction with the androgen receptor and NKX3.1, and down-regulation of PDEF by antiproliferative agents has been associated with reduced PDEF expression. We now report that reduced expression of PDEF leads to a morphologic change, increased migration and invasiveness in prostate cancer cells, reminiscent of transforming growth factor β (TGFβ) function and epithelial-to-mesenchymal transition. Indeed, inhibition of PDEF expression triggers a transcriptional program of genes involved in the TGFβ pathway, migration, invasion, adhesion, and epithelial dedifferentiation. Our results establish PDEF as a critical regulator of genes involved in cell motility, invasion, and adhesion of prostate cancer cells. [Cancer Res 2007;67(9):4219–26]

Introduction

The recent discovery of recurrent chromosomal translocations of the *TMPRSS2* gene to three members of the Ets family, *ERG, ETV1*, and *ETV4*, in the majority of prostate cancer patients has highlighted the relevance of Ets transcription factors for prostate cancer (1, 2). Chromosomal translocations of multiple Ets family members are frequent in various cancer types, including *FLI-1* (3, 4), *ERG* (3, 5), *ETV1* (6), *ETV4* (7), and *FEV*, in Ewing's sarcomas and *TEL/ETV6* in different types of leukemia, fibrosarcoma, lymphoma, and myelodysplastic syndrome (8–10), indicating a critical role for Ets factors in tumorigenesis. Furthermore, deregulated activity of Ets factors is observed in many cancers and apparently contributes not only to tumorigenesis but also to tumor progression, outcome, angiogenesis, epithelial-to-mesenchymal transition (EMT), and metastasis (11). Ets factors act as oncogenes or tumor suppressors *in vitro* and animal models have confirmed their oncogenic activities (11).

Most Ets genes are ubiquitously expressed, but we and others identified recently a group of Ets factors, ESE-1, ESE-2, ESE-3, and PDEF, whose expression is restricted to epithelial cells (12–14). PDEF (SPDEF) is unique among Ets factors because its expression is highly restricted to a small subset of epithelial cell types (i.e., hormone-regulated epithelium, such as prostate, mammary gland, endometrium, and ovary, as well as salivary gland and colon; ref. 12).

The precise function of PDEF in cancer development and progression remains somewhat controversial. Elevated levels of PDEF transcripts have been detected in primary human breast, prostate, and ovarian cancers, as well as breast cancer lymph node metastases, and PDEF transcripts can be detected in peripheral blood of breast cancer patients (15, 16). However, several reports indicate reduced PDEF protein expression in cancer cells relative to their normal counterparts as well as decreased protein expression in invasive, metastatic relative to early-stage breast cancer, possibly due to translational suppression (17).

A potential role for PDEF in cancer cell migration and invasion has emerged, although different investigators have come to opposite conclusions. Whereas, in one study, PDEF overexpression in MDA-MB-231 breast cancer cells inhibits cell growth and reduces invasion and migration (17), in another report, PDEF overexpression induces invasion and migration in breast cancer cells that is further enhanced by mitogen-activated protein kinase–dependent phosphorylation (18). This discrepancy may be due to differences in the cellular environment between different cell lines. A role for PDEF in prostate cancer seems likely due to its involvement in *prostate-specific antigen* (*PSA*) gene regulation and direct interaction with the androgen receptor and the prostate-specific tumor suppressor gene *NKX3.1*, which represses PDEF-mediated activation of the *PSA* promoter in prostate cancer cells (12, 19). However, the precise role of PDEF in prostate cancer has not been explored.

To provide insight into the function of PDEF in prostate cancer and to overcome limitations with overexpression of potentially unphysiologic concentrations of transcription factors, we have used RNA interference (RNAi) experiments to reduce endogenous PDEF expression in prostate cancer cells. We report now that inhibition of PDEF in prostate cancer cells leads to drastic physiologic and morphologic changes that are associated with the conversion of epithelial properties toward mesenchymal phenotypes with decreased epithelial markers, increased mesenchymal markers, and decreased adhesion, enhanced migration, enhanced invasion, and activation of the transforming growth factor β (TGFβ) pathway. We also show that TGFβ represses PDEF expression, indicating that PDEF suppression may mediate part of the biological effects of TGFβ. Thus, PDEF seems to play a critical role in cell motility and invasion of prostate cancer cells, steps that are critical for progression and metastasis of prostate cancer.

Note: Supplementary data for this article are available at Cancer Research Online (http://cancerres.aacrjournals.org/).

Current address for H.H. Otu: Department of Genetics and Bioengineering, Yeditepe University, Istanbul 34755, Turkey.

Requests for reprints: Towia A. Libermann, BIDMC Genomics Center, Beth Israel Deaconess Medical Center and Harvard Medical School, Harvard Institutes of Medicine, 4 Blackfan Circle, Boston, MA 02115. Phone: 617-667-3393; Fax: 617-975-5299; E-mail: tliberma@bidmc.harvard.edu.

doi:10.1158/0008-5472.CAN-06-3689

Materials and Methods

Cell culture. PC-3 and LNCaP prostate cancer cells and the MDA-MB-231 breast cancer cells were grown in Ham's F-12, RPMI 1640, or DMEM (all from BioWhittaker), respectively, supplemented with 10% fetal bovine serum, 50 units/mL penicillin, and 50 μg/mL streptomycin (Life Technologies). Recombinant human TGFβ (7 ng/mL) was purchased from R&D Systems.

Small interfering RNA oligonucleotides and lentivirus vector generation. Three different small interfering RNA (siRNA; Dharmacon, Inc.) for human PDEF [siPDEF1 (5′-AAGAAGGGCAUCAUCCGGAAG-3′), siPDEF2 (5′-AAGUGCUCAAGGACAUCGAGA-3′), and siPDEF3 (5′-AAGCUGCUCAACAUCACCGCA3′)] were evaluated for their abilities to reduce PDEF expression. The most effective PDEF siRNA (siPDEF3) was inserted into a lentivirus vector using a single 83-mer oligonucleotide (5′-CTGTCTAGACAAAAAGTGCTCAAGGACATCGAGATCTCTTGAATCTC-GATGTCCTTGAGCACGGGGATCTGTGGTCTCATACA-3′). For details, see Supplementary Data.

Generation of cell lines stably expressing PDEF siRNA. PC-3 and LNCaP cells were stably infected with the PDEF siRNA or green fluorescent protein (GFP) siRNA lentivirus and enriched as described in Supplementary Data. Protein extracts from sorted cells were analyzed by Western blot using anti-PDEF antibody. These cell lines (PC-3 siGFP, PC-3 siPDEF, LNCaP siGFP, and LNCap siPDEF) were used in all experiments.

Inverted control siRNA design and transient transfection. A scrambled control siRNA [inverted central 8 bp for siPDEF3 (target sequence is 5′-AAGCUACAACUCGUCACCGCA-3′)] was purchased from Dharmacon. RNA (50 μmol/L) duplexes for PDEF (siPDEF2) and scrambled control (siControl) were transfected into PC-3 cells using TKO transfection reagent (Mirus). Forty-eight hours after transfection, RNA was isolated for real-time PCR analysis.

Stable transfection. Wild-type PDEF (PDEF-wt) expression construct was made by subcloning full-length wild type PDEF cDNA into the pCDNA 5′-FLAG expression vector (Invitrogen) to generate pCDNA-PDEF-wt (FLAG-tagged; see Supplementary Data). PC-3 or LNCaP cells (1×10^6) were transfected with 10 μg of each expression vector DNA as described (20). Stably transfected cell pools were selected in G418 (Invitrogen) as PC-3-PDEF-wt and PC-3-FLAG, and LNCaP-PDEF-wt and LNCaP-FLAG.

Construction of adenovirus and adenoviral infection. The FLAG-PDEF–encoding adenovirus was generated as described previously and in more detail in Supplementary Data (21). Recombinant adenoviruses were screened for PDEF expression by Western blot.

Real-time PCR. Total RNA was harvested using QIAshredder (Qiagen) and the RNeasy mini kit (Qiagen). Primers used for real-time PCR and details are described in Supplementary Data.

Western blot analysis. Western blots were done as described in Supplementary Data by using a mouse monoclonal anti-PDEF antibody,[4] mouse anti-vimentin (Santa Cruz Biotechnology), and mouse anti-cytokeratin 18 (Santa Cruz Biotechnology). Mouse anti-tubulin (Santa Cruz Biotechnology) was used as control for loading.

Immunofluorescence. Formaldehyde-fixed, permeabilized cells cultured on glass coverslips were incubated with primary antibodies overnight at 4°C followed by incubation with secondary fluorescent antibodies as described in Supplementary Data. Fluorescent signals for vimentin and cytokeratin 18 were observed with an Alexa Fluor 633–conjugated goat anti-mouse antibody (1:500). F-actin was stained with phalloidin (TRITC labeled; 1:1,000 dilution; Sigma).

Northern blot analysis. Total RNA was analyzed by Northern blotting with a [^{32}P]dUTP-labeled PDEF cDNA probe as described in Supplementary Data.

Microarray analysis. Antisense biotinylated cRNA from 1 μg total RNA harvested from two clones each of PC-3 cells stably expressing PDEF siRNA or GFP siRNA was prepared on the Affymetrix GeneChip Array Station using the GeneChip HT One-Cycle cDNA Synthesis and GeneChip HT IVT Labeling kits (Affymetrix). Biotinylated cRNAs were hybridized to the Affymetrix HT-U133AA of Av2 GeneChip (a high-throughput platform array in 24-well format of HG-U133A). Array washing and staining were done on the GeneChip Array Station following a robotic protocol according to the manufacturer's instructions (Affymetrix). Arrays were scanned on the GeneChip HT scanner (Affymetrix). Signal intensity for each transcript was determined using GeneChip operating software 2.0. The scanned array images were analyzed by dChip (22), which is more robust than Affymetrix Microarray Analysis Suite 5.0 for ~60% of genes (23). We used the lower confidence bound (LCB) >1.2 of the fold change between the two groups as cutoff criteria. The microarray data were uploaded to Gene Expression Omnibus as GSE6576 (GSM152021, GSM152020, GSM152019, and GSM152018). For more details, check Supplementary Data.

Adhesion assays. Ninety-six-well tissue culture plates, coated overnight at 4°C with 50 ng/mL fibronectin, 100 ng/mL Matrigel, or 1% bovine serum albumin (BSA) as negative control, were washed with PBS and blocked for 30 min at 37°C with 250 μg/mL heat-inactivated lipid-free BSA in DMEM. Cells (3×10^4), resuspended in DMEM, were added to the protein-coated wells. After incubation at 37°C for the indicated time course, the wells were washed with PBS, fixed with methanol for 10 min, stained with 0.2% crystal violet in 2% ethanol, and washed thrice with water. The stain was solubilized with 1% SDS and adhesion was quantified by measuring absorbance at 595 nm. BSA-coated wells were used to control for nonspecific adhesion.

Migration and invasion assays. Cell migration and invasion were tested using a modified Transwell chamber migration assay (8-μm pore size membrane, BD Biosciences) or invasion assay (Matrigel-coated membrane, BD Biosciences). Cells (25×10^4) were seeded in serum-free medium into the upper chamber and allowed to migrate or invade toward 10% FCS as a chemoattractant in the lower chamber for 20 h. Cells in the upper chamber were carefully removed using cotton buds, and cells at the bottom of the membrane were fixed and stained with crystal violet. Quantification was done by counting the stained cells.

Luciferase reporter assays. A 1.2-kb PCR fragment of the human Snail2 promoter (AF084243) was inserted into the pGL3-Basic vector (Promega) and designated pSnail2-Luc. To check the effect of PDEF knockdown on transcriptional activity of *Snail2*, pSnail2-Luc or pGL3-Basic vector was transfected into PC-3 siGFP or siPDEF cells together with β-galactosidase control vector in the presence of LipofectAMINE for 16 h. For the effect of TGFβ on transcriptional activity of the *Snail2* promoter, PC-3 cells were transfected with pSnail2-Luc or pGL3-Basic vector together with β-galactosidase control vector. Cells were washed with serum-free medium and incubated in 2 ng/mL TGFβ-containing serum-free medium for 4 h. Lysates were analyzed for luciferase activities using the Dual-Luciferase Reagent Assay kit (Promega) and for expression of the control plasmid (pSVβ-galactosidase) to normalize the luciferase data by the method of Eustice et al. (24). The result for each reporter represents the average of at least three independent assays.

Statistical analysis. Statistical analysis was done using two-tailed unpaired Student's *t* test.

Results

Generation of PDEF knockdown and PDEF-overexpressing prostate cancer cells. Because previous studies evaluating the function of PDEF in cancer cells relied on exogenous overexpression of PDEF by transfection or infection, conclusions from these experiments with some times opposite results have to be considered with some caution. We therefore applied a lentiviral RNAi approach to study the biological role of PDEF in prostate cancer cells. PC-3 prostate cancer cells were stably infected with either the lentivirus encoding PDEF siRNA (PC-3 siPDEF) or a lentivirus encoding siRNA against GFP (PC-3 siGFP) as control. For overexpression experiments, PC-3 cells were generated stably expressing wild type PDEF (PC-3-PDEF-wt) or the control parental

[4] X. Gu et al., unpublished data.

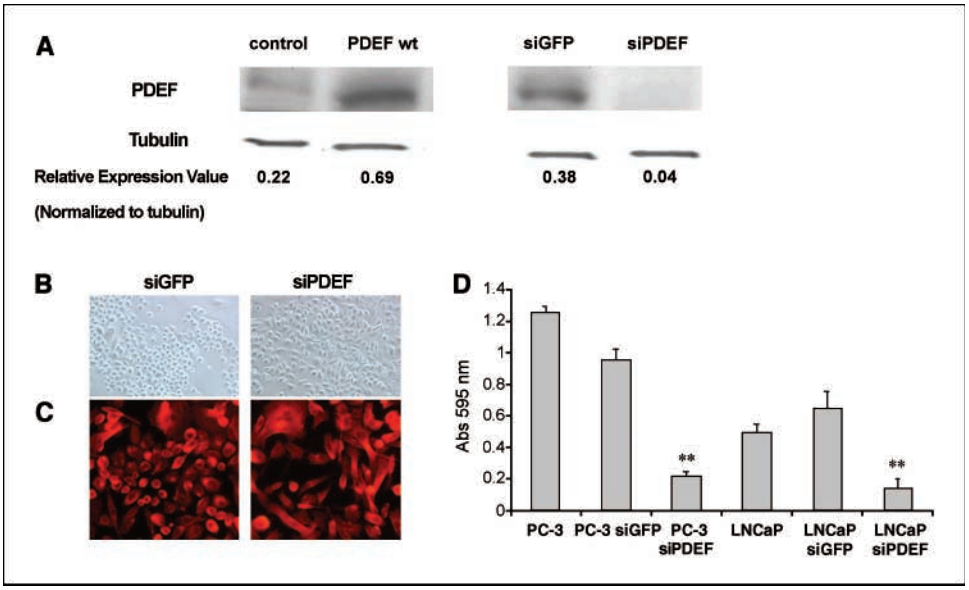

Figure 1. Generation of PC-3 cell lines stably expressing siRNA against PDEF and morphologic and adhesion effects of PDEF siRNA in PC-3 prostate cancer cells. *A,* Western blot analysis using a monoclonal anti-PDEF antibody showing the expression of PDEF in PC-3 cells stably expressing wild type PDEF or siRNA for PDEF compared with control parental vector cells and GFP siRNA-expressing cells. Relative expression levels normalized to tubulin are indicated. *B,* morphologic changes of PC-3 cells, stably infected with the PDEF siRNA or GFP siRNA lentivirus. Magnification, ×200. *C,* filamentous actin and cytoskeletal rearrangements visualized by TRITC-labeled phalloidin. *D,* PDEF knockdown decreases adhesion ability of PC-3 and LNCaP cells. PC-3 or LNCaP cells as well as the cells expressing PDEF siRNA or GFP siRNA were plated on top of collagen gel. Three hours after plating, cells were fixed, stained, and photographed. Adhesion was quantified by A_{595} (absorbance on 595-nm wavelength). The assays were done in triplicate in two independent experiments. Statistical analysis used is two-tailed unpaired Student's *t* test. **, $P < 0.005$.

vector. All experiments were done using at least two cell clones. Western blot analysis of two PC-3 clones from two independent infections or transfections for each construct revealed that lentiviral siRNA expression reduced endogenous PDEF protein expression by 90% compared with GFP siRNA control cells, and wild type PDEF transfection resulted in 3-fold induction of PDEF expression compared with control cells (Fig. 1*A*).

PDEF knockdown causes morphologic changes of PC-3 cells. We investigated whether altering PDEF expression induces morphologic changes. Whereas overexpression of PDEF did not significantly affect morphology of PC-3 cells, loss of PDEF expression by RNAi induced a shape change from rounded epithelial-like cells to fibroblast-like cells with elongated morphologies, a phenotype reminiscent of EMT (Fig. 1*B*). Immunofluorescence with phalloidin revealed significant redistribution of actin cytoskeleton from a cortical ring at cell junction into stress fibers in PC-3 cells expressing PDEF siRNA (Fig. 1*C*).

PDEF knockdown reduces prostate cancer cell adhesion. To explore whether inhibition of PDEF expression affects cellular adhesion, an *in vitro* adhesion assay of siPDEF- or siGFP-expressing PC-3 and LNCaP cells on a matrix of fibronectin or Matrigel was done. PDEF knockdown decreased adhesion of PC-3 cells on Matrigel by 80% ($P < 0.001$) and of LNCaP cells by 70% compared with either control siGFP cells or parental cells ($P = 0.002$; Fig. 1*D*; see representative image in Supplementary Fig. S1). These results show that down-regulation of endogenous PDEF reduces prostate cancer adhesion to extracellular matrix.

PDEF knockdown enhances prostate cancer cell migration and invasion. Because the morphologic changes induced on interference with PDEF expression suggested that those cells had undergone EMT, we evaluated the effect of PDEF knockdown on serum-induced migration of PC-3 cells in a Transwell chamber assay. siPDEF increased the ability of PC-3 cells to migrate through the pores by >50% compared with siGFP-treated cells ($P = 0.041$; Fig. 2*A*). Because cell migration is a process that promotes tumor invasion, we tested the effect of PDEF knockdown on cell invasion using Matrigel-coated Transwell chambers. siPDEF compared with siGFP strongly increased PC-3 cell invasion by 60% after 24-h incubation ($P = 0.042$; Fig. 2*B*). Representative images are shown in Supplementary Fig. S2. Under the same conditions, overexpression of PDEF decreased PC-3 cells invasive ability by 40% ($P = 0.081$; Fig. 2*C*). Similar inhibition of migration and invasion by PDEF overexpression was seen in MDA-MB-231 breast cancer cells. Cells expressing AdPDEF have >60% reduced migration and invasion of cells compared with Ad-FLAG–infected cells (Fig. 2*A* and *B*). We have not used MDA-MB-231 breast cancer cells for siRNA experiments because this cell line does not express endogenous PDEF. These results show that PDEF is an inhibitor of prostate and breast cancer cell migration and invasion.

PDEF regulates genes involved in cell adhesion, integrin signaling, EMT, and vascular endothelial growth factor signaling. To identify PDEF target genes associated with the biological phenotypes, RNAs from siPDEF- and siGFP-expressing PC-3 cells were hybridized to Affymetrix HT U133AAofAv2 GeneChips, which contain >22,000 probe sets. One thousand five hundred eighty-four genes were up-regulated and 1,299 were down-regulated by at least 1.2 LCB of fold change in PC-3 cells expressing siRNA against PDEF. A set of genes shown previously to reflect a transition of epithelial to mesenchymal characteristics was identified. Whereas epithelial markers, E-*cadherin* and *keratins 3, 6a, 6b, 7, 8, 18*, and *19*, were down-regulated, mesenchymal markers, *vimentin*, N-*cadherin*, mesenchymal stem cell antigen, and *CTGF*, as well as inducers of mesenchymal transition, *TGFβ1* and *Snail2*, were up-regulated in PDEF knockdown cells (Fig. 3; Supplementary Table S1). Multiple genes associated with cell adhesion and migration, such as collagens *COL1A1, COL4A1,*

COL4A2, COL4A5, COL4A6, COL5A1, COL5A2, COL6A1, COL6A2, COL6A3, COL13A1, and *COL16A1; syndecan-1* and *syndecan-2; tenascin C; laminin β2* and *γ1; integrins* α_3, α_5, and α_6; and *CDH11*, were up-regulated in PDEF knockdown cells, whereas cytoskeletal and intermediate filament genes as well as *integrins* β_4, β_6, and β_8 were down-regulated, indicating cytoskeletal rearrangements and changes in cell adhesion and migration (Fig. 3; Supplementary Table S1). Modeling of differentially regulated genes identified the integrin signaling pathway as a major target for PDEF (Fig. 3; Supplementary Fig. S3) because, in addition to effects of PDEF on expression of extracellular matrix proteins and integrins, several genes downstream of integrins in the signaling pathway, such as tyrosine kinase focal adhesion kinase (*FAK*)/*PTK, DOCK 1* and *4, RAC2, WASPIP*, and *phosphoinostide 3-kinases PIK3C3* and *PIK3CD*, were up-regulated in PDEF knockdown cells (Supplementary Table S1). These results indicate that inhibition of PDEF expression may lead to integrin receptor aggregation induced by extracellular matrix interaction, which could result in stimulation of signal transduction cascades resulting in cytoskeletal rearrangements and enhanced prostate cancer cell migration. Further, detailed analysis of these signaling pathways on the protein level is needed to support this notion.

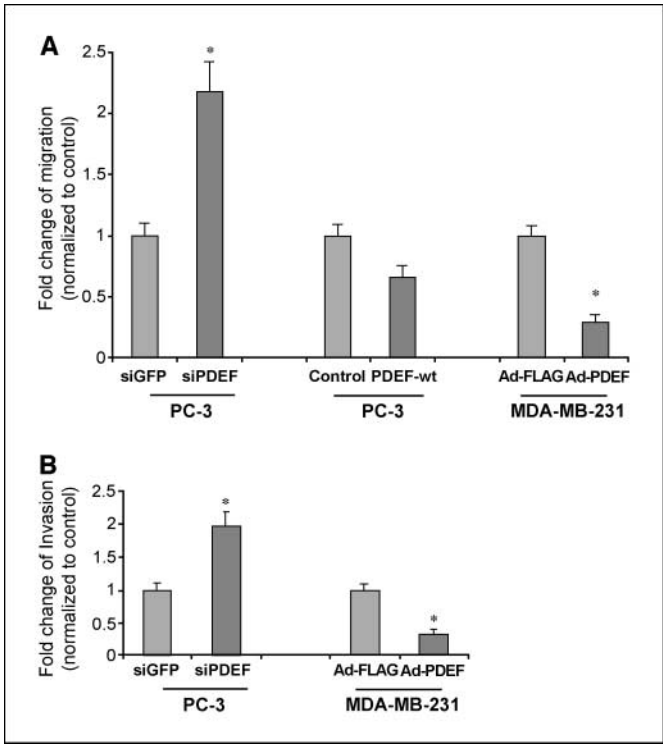

Figure 2. Down-regulation of PDEF results in increased PC-3 cell migration and invasion. *A,* quantification of cells migrating through fibronectin-coated membranes. *Columns,* relative values of cells migrating as a percentage of control. PC-3 cells expressing siGFP or siPDEF, PC-3 cells stably transfected with wild type PDEF expression vector or control vector, and MDA-MB-231 breast cancer cells infected with FLAG-PDEF– or FLAG only–containing adenovirus were cultured on 24-well Transwell plates coated with fibronectin. Sixteen hours later, the cells that migrated through the pores of the membrane to the other side were fixed, stained, and counted. Quantification of cell migration results from three experiments. Statistical analysis used is two-tailed unpaired Student's *t* test. **, $P < 0.005$; *, $P < 0.05$. *B,* quantification of cells invading through Matrigel-coated membranes after 24-h incubation and 10% serum as chemoattractant. *Columns,* relative values of cells invading as a percentage of control. The assays were done in triplicate in two independent experiments. Statistical analysis used is two-tailed unpaired Student's *t* test. *, $P < 0.05$.

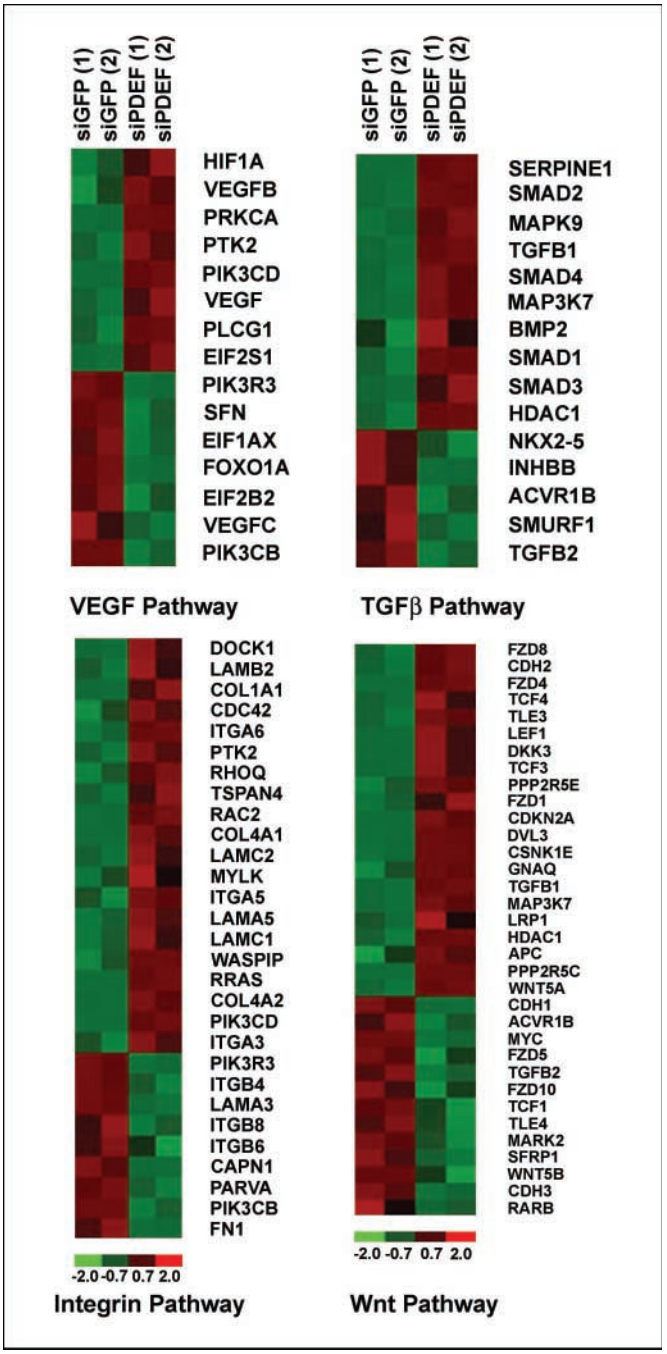

Figure 3. Selected PDEF target genes from transcriptional profiling experiments in PDEF knockdown PC-3 cells. Heatmap of genes in the VEGF, TGFβ, integrin, and Wnt pathways that are targets for PDEF in PC-3 cells. Up-regulated genes in PDEF knockdown cells (*red*) and down-regulated genes (*green*).

Another pathway possibly contributing to enhanced invasion and migration in PDEF knockdown prostate cancer cells is the vascular endothelial growth factor (VEGF) signaling pathway. A transcriptional activator of VEGF, hypoxia-inducible factor-1α, as well as VEGF and VEGFB are up-regulated in PDEF knockdown cells. The VEGF receptor as well as the downstream signaling genes *PI3K, FAK, PLCγ*, and *PKCα* are up-regulated, indicating potential activation (Fig. 3; Supplementary Table S1).

Many biological effects elicited by PDEF knockdown in PC-3 cells and the changes in epithelial and mesenchymal marker

expression are reminiscent of TGFβ signaling. Indeed, the TGFβ-activated *Smad1, Smad2, Smad3*, and *Smad4* transcription factors are up-regulated in PDEF knockdown cells as well as several TGFβ-inducible genes, such as *Snail2* and *plasminogen activator inhibitor-1* (*PAI-1*), a key regulator of tumor invasion and metastasis (Fig. 3; Supplementary Table S1 and Fig. S3). Strikingly, the Wnt/β-catenin pathway, which plays a central role in adhesion and migration, is significantly modulated in PDEF knockdown cells, particularly a strong induction of the downstream transcriptional mediators *LEF-1* and *TCF8*, up-regulation of several catenins, *frizzled homologue 8, dickkopf homologue 3,* and *Wnt5a*, and down-regulation of E-cadherin (Fig. 3; Supplementary Table S1). These results show that PDEF suppresses tumor cell invasion and migration via modulating multiple signaling pathways.

Functional annotation of differentially expressed genes. To investigate the biological processes deregulated in PDEF knockdown PC-3 cells, we implemented an enrichment analysis of all differentially expressed genes (1,584 up and 1,299 down) using the database for annotation, visualization, and integrated discovery (DAVID; ref. 25). DAVID is useful to identify enriched biological themes, functional clusters of genes. Clusters of biological processes, keywords, terms, functions, and pathways with enrichment scores of >2 against all human genes as background are listed in Supplementary Table S2. One of the top categories identified includes signaling pathways relevant to cell invasion, adhesion, migration, and invasion (see colorgrams in Supplementary Fig. S4). The colorgrams include enriched genes involved in the Wnt, VEGF, integrin, and TGFβ pathways (Supplementary Fig. S5).

Blocking PDEF expression in PC-3 cells results in loss of epithelial markers and induction of mesenchymal markers. Various genes linked to mesenchymal/migratory cells as described above were induced on PDEF depletion. Furthermore, genes associated with epithelial cells and known or suspected to be lost

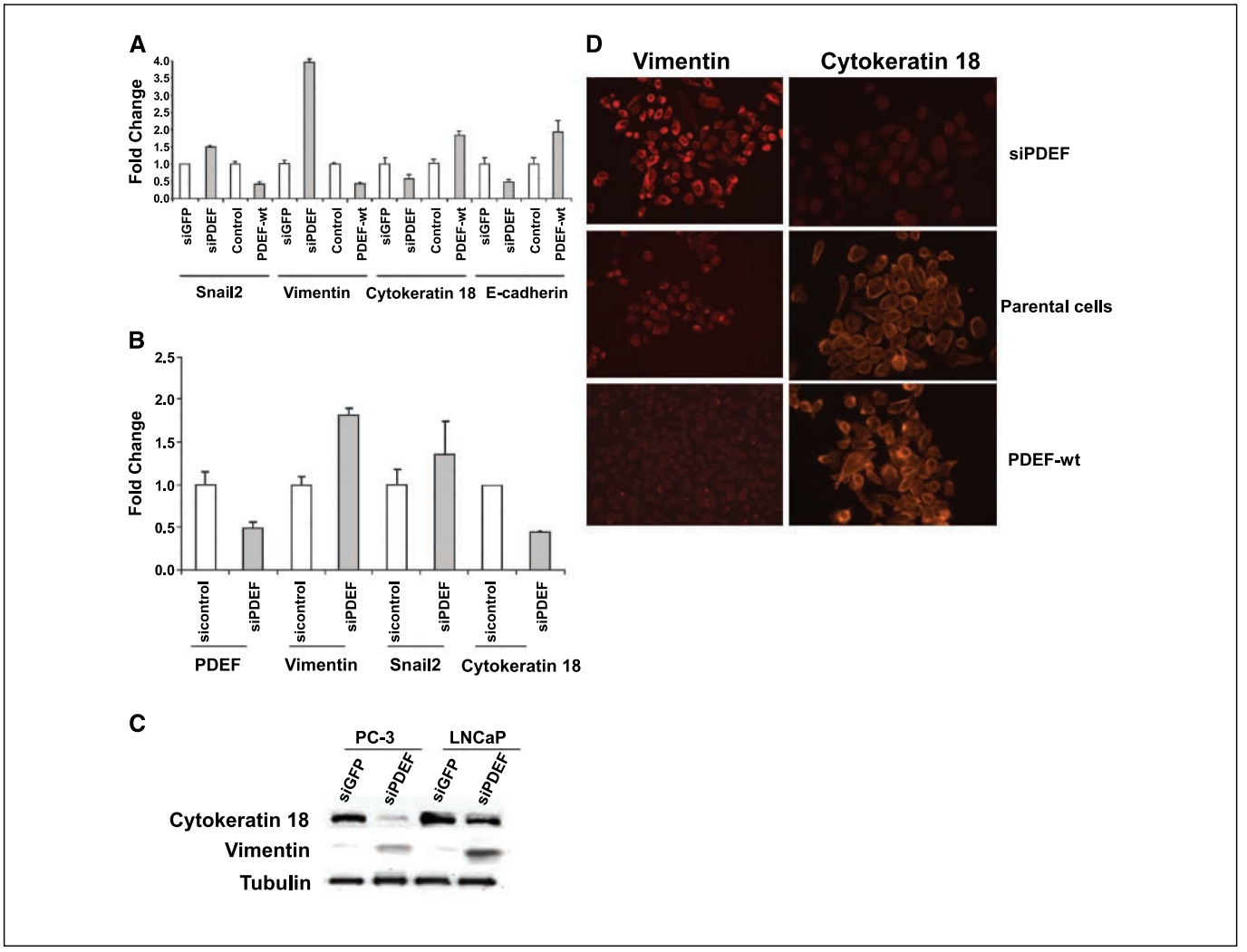

Figure 4. EMT markers regulated by PDEF in PC-3 cells. *A,* real-time PCR analysis of Snail2, vimentin, cytokeratin 18, and E-cadherin in PC-3 cells with different PDEF expression levels. Total RNA was collected from PC-3 cell stably expressing siRNA for GFP or PDEF, or wild type PDEF, and control vector. Each RNA was normalized to glyceraldehyde-3-phosphate dehydrogenase (GAPDH). *B,* expression of PDEF, vimentin, Snail2, and cytokeratin 18 by real-time PCR was detected in PC-3 cells transiently transfected with second siRNA for PDEF (siPDEF2) or an inverted control siRNA. Each RNA expression was normalized to GAPDH. *C,* Western blot analysis for cytokeratin 18 and vimentin in PC-3 and LNCaP cells (24 h in culture) stably expressing siRNA against PDEF or GFP. Tubulin levels were analyzed as a control protein, the levels of which were not expected to change during EMT. *D,* immunostaining of vimentin and cytokeratin 18 in PC-3 stably expressing siPDEF, PDEF-wt, or parental cells.

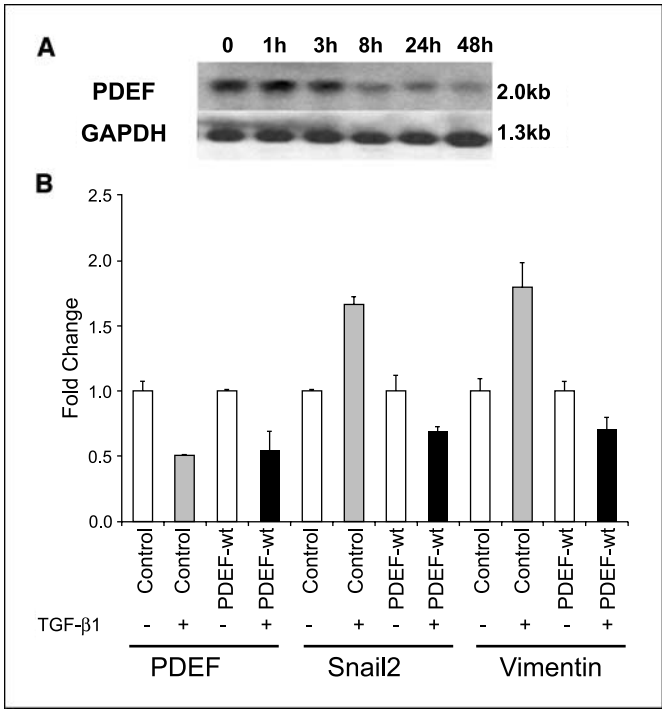

Figure 5. PDEF is a downstream target of TGFβ. *A,* Northern blot analysis of PDEF expression in LNCaP cells cultured in serum-free medium with TGFβ for different times. Northern blots were probed with [^{32}P]dUTP-labeled PDEF cDNA. A GAPDH probe was used for equal loading. *B,* PDEF overexpression in PC-3 cells inhibits the TGFβ effects on EMT markers. PC-3 cells overexpressing PDEF and control cells were starved in serum-free medium overnight and then stimulated with 7 ng/mL TGFβ for 3 d. Real-time PCR for vimentin, fibronectin, and Snail2, in the absence or presence of TGFβ.

during EMT, such as E-cadherin, plakoglobin, and cytokeratins, were down-regulated in PC-3 siPDEF cells. We validated expression of several classic markers of EMT, including vimentin, Snail2, cytokeratin 18, and E-cadherin, by real-time PCR in PDEF knockdown and PDEF-overexpressing PC-3 cells. Whereas Snail2 and vimentin were induced by siRNA against PDEF, overexpression of PDEF reduced expression of these genes (Fig. 4*A*). In contrast, cytokeratin 18 and E-cadherin were down-regulated in PDEF knockdown cells, and expression increased in PDEF-overexpressing cells (Fig. 4*A*), further supporting the conclusions from the previous experiments. Similar effects of PDEF on vimentin and E-cadherin expression were seen in another prostate cancer cell line, LNCaP, as well as in two breast cancer cell lines, SKBr-3 and MCF-7. The specificity of PDEF siRNA oligonucleotides and of the effect of knocking down PDEF was validated by transient transfection of scrambled oligonucleotides (siControl, inverted central 8 bp of the specific siRNA) and a second siRNA against PDEF (siPDEF2) into PC-3 cells. RT-PCR analysis 48 h after transfection (Fig. 4*B*) confirmed that expression of PDEF and cytokeratin 18 was decreased by siPDEF2 only, whereas Snail2 and vimentin were induced.

PDEF-dependent changes in mRNA expression led to equivalent changes in protein expression as analyzed by Western blotting. Cytokeratin 18 protein levels decreased and vimentin protein levels increased in PDEF knockdown PC-3 and LNCaP cells (Fig. 4*C*). Immunofluorescence analysis confirmed a loss of the epithelial marker cytokeratin 18 in PDEF knockdown cells and an increase of the mesenchymal marker vimentin, whereas PDEF-overexpressing cells did not stain for vimentin and stained stronger for cytokeratin 18 (Fig. 4*D*). Moreover, control PC-3 cells expressing siGFP and parental PC-3 cells stained faintly for vimentin and intermediate for cytokeratin 18.

TGFβ reduces expression of PDEF in prostate cancer cells. Because PDEF inhibition induces phenotypic changes similar to TGFβ action and modulated expression of TGFβ target genes, we evaluated whether PDEF may be downstream of TGFβ. Northern blot analysis of TGFβ-stimulated LNCaP (Supplementary Fig. S6) and PC-3 (Fig. 5*A*) cells indicates decreased PDEF expression in TGFβ-treated cells in a time-dependent manner, starting 8 h after stimulation (Fig. 5*A*). Real-time PCR confirmed down-regulation of PDEF expression by TGFβ stimulation (Fig. 5*B*).

Repression of PDEF expression is required for induction of mesenchymal genes by TGFβ. To determine whether PDEF repression is required for TGFβ induction of mesenchymal genes, PC-3 cells overexpressing PDEF were stimulated with TGFβ for 3 days. Real-time PCR showed that TGFβ induced expression of vimentin and Snail2 in control PC-3 cells transfected with the parental vector, whereas induction of these genes by TGFβ was completely inhibited in PDEF-overexpressing cells (Fig. 5*B*). These data most vividly show that PDEF repression is mediating at least some of the biological effects of TGFβ.

PDEF and TGFβ regulate transactivation of the Snail2 promoter. Snail2, in addition to being a mesenchymal marker, represses expression of E-cadherin and is a critical regulator of EMT (26). To determine whether PDEF and TGFβ affect Snail2 transcription, we inserted the 1.2-kb human Snail2 promoter upstream of the luciferase reporter gene into the pGL3 vector. Analysis of the Snail2 promoter sequence identified several potential PDEF binding sites (consensus sequence: GGAA/T) and Smad binding sites (consensus sequence: AGAC) in the 1.2-kb

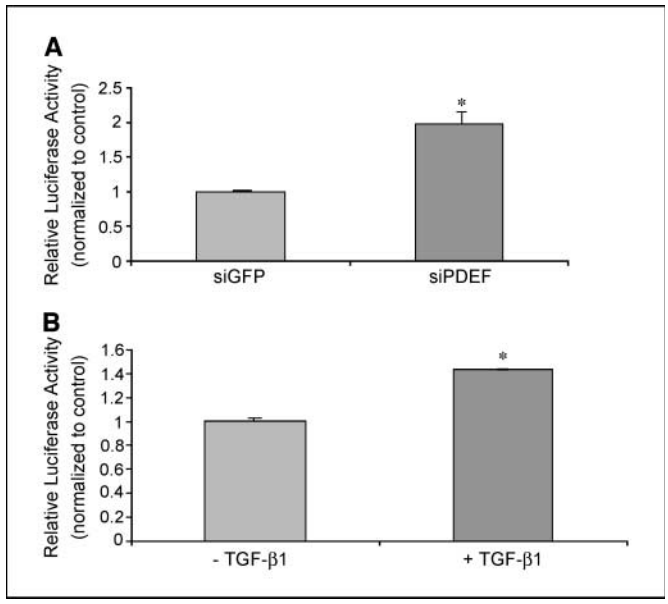

Figure 6. TGFβ and knockdown of PDEF enhance Snail2 transcription at the promoter level. *A,* luciferase reporter assays of siGFP- and siPDEF-expressing PC-3 cells transfected with 600 ng pGL3 or pGL3-Snail2 promoter were done as described. *B,* 600 ng pGL3 or pGL3-Snail2 promoter was transfected into PC-3 cells. Sixteen hours following transfection, cells were switched to serum-free medium with or without 2 ng/mL TGFβ and incubated for an additional 6 h. Luciferase activity was determined as described. Statistical analysis used is two-tailed unpaired Student's *t* test. *, $P < 0.05$.

Snail2 promoter (Supplementary Fig. S7). PC-3 cells containing either siPDEF or siGFP were transiently transfected with either the Snail2 promoter luciferase vector or the parental pGL3 vector, and luciferase activity was read 24 h after transfection. Activity of the Snail2 promoter increased ~2.0-fold ($P < 0.05$) in PC-3 with siPDEF compared with siGFP (Fig. 6*A*), correlating with the Snail2 expression data. Similarly, TGFβ treatment of PC-3 cells transfected with the luciferase vectors increased Snail2 promoter activity ~1.5-fold ($P < 0.05$; Fig. 6*B*).

Discussion

Our original discovery of PDEF as an epithelial-specific Ets transcription factor involved in prostate cancer–specific *PSA* gene expression indicated a critical role for PDEF in prostate cancer (12). Further publications confirmed the role of PDEF and showed that the prostate cancer–specific tumor suppressor NKX3.1 directly interacts with PDEF and thereby inhibits PDEF-mediated PSA promoter transactivation (19). Additional reports suggest that PDEF protein expression, in contrast to mRNA expression, is reduced in prostate cancer cells relative to normal prostate epithelium. Similarly, the role of PDEF in breast cancer remains controversial. Whereas several publications suggest that PDEF is a marker for metastatic breast cancer, PDEF mRNA is up-regulated in breast cancer epithelium relative to normal mammary epithelium throughout tumor progression, and PDEF overexpression in MCF-10A breast epithelial cells coexpressing the receptor tyrosine kinases (RTK) ErbB2 and colony-stimulating factor-1 (CSF-1) receptor/CSF-1 induces migration and invasion of breast cancer cells (18), other reports indicate reduced PDEF protein expression in advanced breast cancer and inhibition of migration and invasion in breast cancer cells overexpressing PDEF (17).

Whereas previous publications relied on overexpression experiments to determine biological function of PDEF, we have focused our effort on reducing expression of endogenous PDEF by RNAi to evaluate the role of PDEF in prostate cancer and only apply overexpression when necessary to show the opposite effect of reducing PDEF expression. Our results show that inhibition of endogenous PDEF expression in PC-3 cells results in alterations of cell morphology with increased motile-invasive activities concomitant with changes in epithelial and mesenchymal marker gene expression as well as pleiotropic responses in multiple signaling pathways associated with adhesion, migration, and invasion of cancer cells. Thus, our data indicate that PDEF expression reduces motility and invasion and enhances adhesion of prostate cancer cells. Our data are consistent with published reports by Feldman et al. (17) on the inhibitory role of overexpressed PDEF in breast cancer cell migration and the role of the PDEF *Drosophila* homologue D-Ets4 as an inhibitor of migration of primordial germ cells (27). Our results, nevertheless, do not rule out that PDEF in response to RTKs and extracellular signal-regulated kinase activation switches from an inhibitor of migration into an activator of migration as suggested by the results from Gunawardane et al. (18), suggesting a bimodal function of PDEF that may be modulated both by regulation on the protein expression level and by phosphorylation.

Some biological responses elicited on interference with PDEF expression are reminiscent of EMT and TGFβ function (28). TGFβ plays a major role in human cancer, including prostate cancer, and functions as both a tumor suppressor in early tumorigenesis and a tumor promoter during tumor progression (29). TGFβ is frequently overexpressed in hormone-refractory prostate cancer and a risk factor for tumor progression and poor clinical outcome (30, 31). During tumor progression, TGFβ induces EMT, tumor cell migration, and invasion by enhancing expression of mesenchymal genes, extracellular matrix proteins, cell adhesion proteins, and proteases, thus promoting the metastatic potential of cancer cells (32–34). TGFβ function is critically involved in epithelial dedifferentiation toward mesenchymal cells by activating transcriptional repressors of the Snail family that inhibit epithelial-specific E-cadherin expression (35, 36). Our data show that TGFβ reduces PDEF expression and reduced PDEF expression affects expression of various TGFβ target genes, including *Smads*, which mediate TGFβ responses, *vimentin, Snail2, fibronectin*, and various extracellular matrix and adhesion proteins. Because PDEF overexpression blocks the TGFβ effect on expression of several critical target genes, PDEF may play an important role in TGFβ signaling and cancer cell migration.

Although EMT plays a critical role in progression and metastasis of various cancer types, EMT per se has not been typically observed in prostate cancer. Nevertheless evidence of EMT-like changes exists in prostate cancer cell lines and during prostate cancer progression. Overexpression of PSA or kallikrein 4 in PC-3 cells induces cell migration through Matrigel and a morphologic change from rounded epithelial-like to spindle-shaped, mesenchymal-like cells concomitant with a decrease in adhesion (37). This EMT-like phenotype is associated with decreased E-cadherin and increased vimentin expression (37). In contrast, overexpression of the Wnt inhibitor Frzb/secreted Frizzled-related protein 3 in PC-3 cells leads to induction of epithelial markers, such as E-cadherin, and decrease in mesenchymal markers vimentin and fibronectin resulting in reduced invasive capacity (38). These results are highly reminiscent of our own observations with regard to PDEF knockdown, and our transcriptional profiling data implicate Wnt and TGFβ pathways in PDEF function. Our transcriptional profiling analysis shows up-regulation of several positive regulators or mediators of the Wnt signaling pathway, such as WNT5A, TGFβ1, LEF1, TCF3, TCF4, FZD1, FZD4, and FZD8, and down-regulation of negative regulators, such as SFRP1, in PDEF knockdown cells, indicating that PDEF expression may inhibit Wnt signaling. Nevertheless, some positive regulators are down-regulated rather than up-regulated, showing the complexity of effects and the caution to overinterpret microarray data without further protein analysis. Nevertheless, an indication of activation of Wnt signaling is the high up-regulation of the downstream target LEF1. Motility and metastatic potential of prostate cancer cell lines directly correlates with vimentin expression levels and high vimentin expression in tissue sections correlates with poorly differentiated prostate cancers and bone metastases (39, 40). E-cadherin loss correlates with increased Gleason scores, increased invasive capacity, extracapsular dissemination, and bone metastasis (41, 42). Thus, there is a clear shift on prostate cancer progression and metastasis from a well-differentiated, epithelial phenotype expressing E-cadherin to a poorly differentiated, mesenchymal, invasive phenotype expressing vimentin. Our data implicate PDEF in these processes. Additionally, our results indicate involvement of PDEF in multiple biological pathways implicated in cancer development and progression. In the integrin signaling pathway, genes associated with cell adhesion and migration, such as the collagens *COL1A1, COL4A1*, and *COL4A2* and integrins *ITGA6, ITGA5*, and *ITGA3*, as well as the positive signaling regulators *FAK* (*PTK2*), *MYLK, WASPIP, RAC2, RHOQ*, and *RRAS*, are up-regulated in

PDEF knockdown cells, suggesting that PDEF expression leads to inhibition of the integrin pathway resulting in reduced cancer cell motility.

In summary, our data indicate that PDEF is a downstream target of TGFβ and repression of PDEF expression is a critical step for TGFβ to elicit its biological effects in prostate cancer cells, apparently via activation of several signaling pathways (Wnt, VEGF, and integrin) linked to adhesion, migration, invasion, and EMT.

Acknowledgments

Received 10/6/2006; revised 1/5/2007; accepted 2/22/2007.

Grant support: NIH grant 1RO1 CA85467 and Department of Defense grant PC001420 (T.A. Libermann), HMS Fund for Women's Health (X. Gu), and Department of Defense grant PC051217 (L.F. Zerbini).

The costs of publication of this article were defrayed in part by the payment of page charges. This article must therefore be hereby marked *advertisement* in accordance with 18 U.S.C. Section 1734 solely to indicate this fact.

We thank Dr. Inder M. Verma for help with generation of LV-siRNA PDEF.

References

1. Tomlins SA, Rhodes DR, Perner S, et al. Recurrent fusion of TMPRSS2 and ETS transcription factor genes in prostate cancer. Science 2005;310:644–8.

2. Tomlins SA, Mehra R, Rhodes DR, et al. TMPRSS2:ETV4 gene fusions define a third molecular subtype of prostate cancer. Cancer Res 2006;66:3396–400.

3. Im YH, Kim HT, Lee C, et al. EWS-FLI1, EWS-ERG, EWS-ETV1 oncoproteins of Ewing tumor family all suppress transcription of transforming growth factor β type II receptor gene. Cancer Res 2000;60:1536–40.

4. Prieur A, Tirode F, Cohen P, Delattre O. EWS/FLI-1 silencing and gene profiling of Ewing cells reveal downstream oncogenic pathways and a crucial role for repression of insulin-like growth factor binding protein 3. Mol Cell Biol 2004;24:7275–83.

5. Shing DC, McMullan DJ, Roberts P, et al. FUS/ERG gene fusions in Ewing's tumors. Cancer Res 2003;63: 4568–76.

6. Khoury JD. Ewing sarcoma family of tumors. Adv Anat Pathol 2005;12:212–20.

7. Ishida S, Yoshida K, Kaneko Y, et al. The genomic breakpoint and chimeric transcripts in the EWSR1–4/E1AF gene fusion in Ewing sarcoma. Cytogenet Cell Genet 1998;82:278–83.

8. Stams WA, den Boer ML, Beverloo HB, et al. Expression levels of TEL, AML1, and the fusion products TEL-AML1 and AML1-TEL versus drug sensitivity and clinical outcome in t(12;21)-positive pediatric acute lymphoblastic leukemia. Clin Cancer Res 2005;11:2974–80.

9. Bohlander SK. ETV6: a versatile player in leukemogenesis. Semin Cancer Biol 2005;15:162–74.

10. Hock H, Meade E, Medeiros S, et al. Tel/Etv6 is an essential and selective regulator of adult hematopoietic stem cell survival. Genes Dev 2004;18:2336–41.

11. Hsu T, Trojanowska M, Watson DK. Ets proteins in biological control and cancer. J Cell Biochem 2004;91: 896–903.

12. Oettgen P, Finger E, Sun Z, et al. PDEF, a novel prostate epithelium-specific ets transcription factor, interacts with the androgen receptor and activates prostate-specific antigen gene expression. J Biol Chem 2000;275: 1216–25.

13. Oettgen P, Kas K, Dube A, et al. Characterization of ESE-2, a novel ESE-1-related Ets transcription factor that is restricted to glandular epithelium and differentiated keratinocytes. J Biol Chem 1999;274:29439–52.

14. Kas K, Finger E, Grall F, et al. ESE-3, a novel member of an epithelium-specific ets transcription factor subfamily, demonstrates different target gene specificity from ESE-1. J Biol Chem 2000;275:2986–98.

15. Ghadersohi A, Sood AK. Prostate epithelium-derived Ets transcription factor mRNA is overexpressed in human breast tumors and is a candidate breast tumor marker and a breast tumor antigen. Clin Cancer Res 2001;7:2731–8.

16. Ghadersohi A, Odunsi K, Lele S, et al. Prostate derived Ets transcription factor shows better tumor-association than other cancer-associated molecules. Oncol Rep 2004;11:453–8.

17. Feldman RJ, Sementchenko VI, Gayed M, Fraig MM, Watson DK. Pdef expression in human breast cancer is correlated with invasive potential and altered gene expression. Cancer Res 2003;63:4626–31.

18. Gunawardane RN, Sgroi DC, Wrobel CN, Koh E, Daley GQ, Brugge JS. Novel role for PDEF in epithelial cell migration and invasion. Cancer Res 2005;65:11572–80.

19. Chen H, Nandi AK, Li X, Bieberich CJ. NKX-3.1 interacts with prostate-derived Ets factor and regulates the activity of the PSA promoter. Cancer Res 2002;62: 338–40.

20. Gu X, Shin BH, Akbarali Y, et al. Tel-2 is a novel transcriptional repressor related to the Ets factor Tel/ETV-6. J Biol Chem 2001;276:9421–36.

21. Zerbini LF, Wang Y, Cho JY, Libermann TA. Constitutive activation of nuclear factor κB p50/p65 and Fra-1 and JunD is essential for deregulated interleukin 6 expression in prostate cancer. Cancer Res 2003;63:2206–15.

22. Li C, Wong WH. Model-based analysis of oligonucleotide arrays: expression index computation and outlier detection. Proc Natl Acad Sci U S A 2001;98:31–6.

23. Barash Y, Dehan E, Krupsky M, et al. Comparative analysis of algorithms for signal quantitation from oligonucleotide microarrays. Bioinformatics 2004;20: 839–46.

24. Eustice DC, Feldman PA, Colberg-Poley AM, Buckery RM, Neubauer RH. A sensitive method for the detection of β-galactosidase in transfected mammalian cells. Biotechniques 1991;11:739–40, 742–3.

25. Dennis G, Jr., Sherman BT, Hosack DA, et al. DAVID: Database for annotation, visualization, and integrated discovery. Genome Biol 2003;4:P3.

26. Moreno-Bueno G, Cubillo E, Sarrio D, et al. Genetic profiling of epithelial cells expressing e-cadherin repressors reveals a distinct role for snail, slug, and e47 factors in epithelial-mesenchymal transition. Cancer Res 2006;66:9543–56.

27. Hsouna A, Watson DK, Hsu T. Developmental expression pattern of D-ets4, the *Drosophila* homologue of human Pdef. Gene Expr Patterns 2004;5: 285–9.

28. Ellenrieder V, Hendler SF, Boeck W, et al. Transforming growth factor β1 treatment leads to an epithelial-mesenchymal transdifferentiation of pancreatic cancer cells requiring extracellular signal-regulated kinase 2 activation. Cancer Res 2001;61:4222–8.

29. Bello-DeOcampo D, Tindall DJ. TGF-βl/Smad signaling in prostate cancer. Curr Drug Targets 2003;4: 197–207.

30. Patel BJ, Pantuck AJ, Zisman A, et al. CL1-GFP: an androgen independent metastatic tumor model for prostate cancer. J Urol 2000;164:1420–5.

31. Sokoloff MH, Tso CL, Kaboo R, et al. *In vitro* modulation of tumor progression-associated properties of hormone refractory prostate carcinoma cell lines by cytokines. Cancer 1996;77:1862–72.

32. Giannelli G, Bergamini C, Fransvea E, Sgarra C, Antonaci S. Laminin-5 with transforming growth factor-β1 induces epithelial to mesenchymal transition in hepatocellular carcinoma. Gastroenterology 2005;129: 1375–83.

33. Han G, Lu SL, Li AG, et al. Distinct mechanisms of TGF-β1-mediated epithelial-to-mesenchymal transition and metastasis during skin carcinogenesis. J Clin Invest 2005;115:1714–23.

34. Nakajima S, Doi R, Toyoda E, et al. N-cadherin expression and epithelial-mesenchymal transition in pancreatic carcinoma. Clin Cancer Res 2004;10:4125–33.

35. Valdes F, Alvarez AM, Locascio A, et al. The epithelial mesenchymal transition confers resistance to the apoptotic effects of transforming growth factor β in fetal rat hepatocytes. Mol Cancer Res 2002;1:68–78.

36. Gotzmann J, Huber H, Thallinger C, et al. Hepatocytes convert to a fibroblastoid phenotype through the cooperation of TGF-β1 and Ha-Ras: steps towards invasiveness. J Cell Sci 2002;115:1189–202.

37. Veveris-Lowe TL, Lawrence MG, Collard RL, et al. Kallikrein 4 (hK4) and prostate-specific antigen (PSA) are associated with the loss of E-cadherin and an epithelial-mesenchymal transition (EMT)-like effect in prostate cancer cells. Endocr Relat Cancer 2005;12:631–43.

38. Zi X, Guo Y, Simoneau AR, et al. Expression of Frzb/secreted Frizzled-related protein 3, a secreted Wnt antagonist, in human androgen-independent prostate cancer PC-3 cells suppresses tumor growth and cellular invasiveness. Cancer Res 2005;65:9762–70.

39. Nukui F, Nagata M, Kurokawa J, et al. A case of osteosarcoma in pelvic bone following radiation therapy for prostate cancer. Nippon Hinyokika Gakkai Zasshi 2004;95:59–62.

40. de Pinieux G, Legrier ME, Poirson-Bichat F, et al. Clinical and experimental progression of a new model of human prostate cancer and therapeutic approach. Am J Pathol 2001;159:753–64.

41. Dunsmuir WD, Gillett CE, Meyer LC, et al. Molecular markers for predicting prostate cancer stage and survival. BJU Int 2000;86:869–78.

42. Bryden AA, Hoyland JA, Freemont AJ, et al. E-cadherin and β-catenin are down-regulated in prostatic bone metastases. BJU Int 2002;89:400–3.